

よって、2週間連続してHbVに造血幹・前駆細胞が曝されるという状況はヒトの臨床例では想定できないし、むしろ1-3日間曝されるというのが想定できる期間である。さらにin vivoでは、HbVはマクロファージ内に蓄積しており、in vitroのようにHbVと造血幹・前駆細胞が直接相互作用をすることは極めて少ないと考えられる。従って造血幹・前駆細胞が直接1-3日間HbVに曝露される場合において、造血前駆細胞の活性に大きな影響がなかったという結果は、HbVをヒトに投与した場合、造血に大きな悪影響を及ぼす可能性が極めて少ないことを支持するものと捉えることができる。

国外では、ヘモグロビンを基盤とし化学修飾させたセルフリ型的人工酸素運搬体の開発が進められている。これらの修飾ヘモグロビンや分子内架橋を行ったヘモグロビンは、我々と同じようにヒト臍帯血から調製したCD34陽性細胞を用いた液体培養系において、赤芽球前駆細胞の増殖の亢進を促すと報告されている<sup>28</sup>。また、AIDSの治療に用いられる薬剤3'-azido-3'-deoxythymidine (AZT)による造血抑制を、ヘモグロビンおよび化学修飾ヘモグロビンがin vitro, in vivoの両方で回復させる(但し赤血球造血に特異的)ことが示され<sup>29,30</sup>、これらの赤血球造血作用は酸素運搬能以外の付加価値と位置付けられている。修飾ヘモグロビンのこれらのin vitroでの作用は、赤芽球系前駆細胞が修飾ヘモグロビンを取り込み、赤血球造血作用のあるhemeに分解するためと推測されている<sup>30</sup>。HbVの場合は、赤芽球系前駆細胞を含めて造血前駆細胞の増殖亢進作用はみられず、逆に長期間では抑制する結果となったが、その機序は現時点では明らかでない。少なくとも赤芽球系前駆細胞は、HbVを修飾ヘモグロビンのようには容易には取り込まないと考えられる。

#### 4. ヘモグロビン小胞体の補体系、凝固系、カリクレイン-キニン系に対する影響

リポソームは細胞膜と同様リン脂質を構成成分としているが、生体にとっては異物であり、血液細胞のみならず血漿タンパク質と相互作用する<sup>31</sup>。この作用は、リポソームの大きさ、荷電、構成脂質、さらにリポソーム自体への化学修飾により異なってくる。リポソームの中で陰性荷電のものは、ラット、モルモット、そしてヒトの補体を活性化することが広く知られている<sup>32-34</sup>。その結果、オプソニン化したリポソームは、細網内皮系により循環血液中から速やかに排除される。また陰性荷電リポソームは凝固系第7因子を活性化させ、内因系の凝固カスケードならびにカリクレイン・キニン系活性のトリガーとなる<sup>35,36</sup>。リポソームの構成成分のコレステロール含量も補体の活性化に影響することが知られ、この活性化は血液中の自然抗体によると考えられている<sup>34,37,38</sup>。これまで述べてきたリポソーム包埋型ヘモグロビンにおいても、ヒトの血液中の脂質に対する自然抗体によって、古典経路と第二経路の両方を介して補体の活性化が惹起される<sup>39</sup>。さらに、ブタモデル実験においては、ある種のリポソームによって偽アレルギー反応が起こり、補体活性化との関連が考えられている<sup>40-42</sup>。一方、リポソーム

をPEG修飾することで、これらの反応を防ぐことができることが報告されている<sup>43-45</sup>。しかしながら、リポソーム包埋型ヘモグロビンのみならず抗がん剤doxorubicinを封入したPEG修飾リポソームDoxil/Caelyxにおいても、顔面紅潮、呼吸困難、紅斑、胸痛、背骨痛、血圧低下または血圧上昇が報告されている<sup>46-48</sup>。またこれらの症状はdoxorubicin自体では起こらないため、リポソームによるものと考えられている<sup>49</sup>。したがってHbVの生体適合性を評価するうえで、ヒトの補体系、凝固系、カリクレイン-キニン系に対する影響を検討することの意義は大きいと考えられた。

この検討においては、DHSGをそのリポソーム構成成分としPEG修飾された現行のHbV (DHSG-HbV)、DPPGを構成成分としPEG修飾されたHbV (DPPG-HbV)、DPPGを構成成分とするがPEG未修飾のHbV (DPPG-HbV (no PEG))、強陰性荷電PEG未修飾リポソーム (EL-A)を用いた<sup>50</sup>。なお、EL-Aの脂質構成はDPPC:CHOL:DPPG (30:40:30) (mol%)からなり、その生理食塩水中でのゼータ電位は-47.2mVであった<sup>50</sup>。

HbVを健康人ヒト血清と20%あるいは40%で混合し、37℃にて24時間インキュベーション後、遠心により各種HbVを除去し、その上清の補体価(CH50)を測定した。Table 4に示すように、DHSG-HbVを混合することによって血清が希釈されるためCH50は低下した。強陰性荷電PEG未修飾リポソーム(EL-A)を添加した群では著しいCH50の低下がみられるのに対し、DHSG-HbVを20%あるいは40%で添加した群では、それぞれ生食を添加した場合のCH50より減少することはなかった。さらに3種のHbVと比較してみると(Table 5)、DHSG-HbVとDPPG-HbVは、補体消費を起こさなかったのに対し、DPPG-HbV (no PEG)は40%の添加によってほぼ完全に補体が消費された。以上の結果から、現行のDHSG-HbVおよびPEG修飾されたDPPG-HbVは、ヒト血清補体系を活性化しないと考えられた。

Table 4. Consumption of complement by HbV and Liposome.

Additive	CH50 (U/mL)	
	(additive:serum)	
	20:80	40:60
Saline	33.4 ± 2.8	21.4 ± 1.7
DHSG-HbV	33.5 ± 2.9	22.9 ± 2.4
EL-A	25.1 ± 2.7*	5.9 ± 0.7*

The complement titer (CH50) was measured using a 50% hemolysis assay with a commercial kit. DHSG-HbV, saline or Coatsome EL-A (a negative-charged liposome) were mixed with serum as indicated ratio (v/v) at 37°C for 24 hr. The lipid composition (mol%) of Coatsome EL-A was DPPC:CHOL:DPPG=30:40:30. Data are represented as the mean ± SD using serum from five individuals. The CH50 of 100% serum was 38 ± 3.2 U/mL. \*p < 0.05 vs. saline.

Table 5. Consumption of complement by various types of HbV.

Additive	CH50 (U/mL)	
	(additive:serum)	
	20:80	40:60
Saline	36.4	27.9
DHSG-HbV	37.6	31.4
DPPG-HbV	35.9	28.4
DPPG-HbV(no PEG)	29.9	Under detection limit

The complement titer (CH50) was measured using a 50% hemolysis assay with a commercial kit. DHSG-HbV, DPPG-HbV, DPPG-HbV (no PEGylation) or saline were mixed with serum as indicated ratio (V/V) at 37 °C for 24 hr. The CH50 of 100% serum was 45.1 U/mL.

次に凝固系に及ぼす影響をこれら3種のリポソーム構成成分の異なるHbVを用い、プロトロンビン時間(PT)および活性化部分トロンボプラスチン時間(APTT)について比較した。PTは健康人ヒト血漿との混合比率が上昇するにつれて凝固時間が遅延した。血漿に対し生食の比が20%および60%においては、これら3種のHbVはいずれも生食添加の場合のPT時間を有意に短縮させたが、その差は1秒以内であった。APTT時間に対し、DPPG-HbVとDPPG-HbV(no PEG)は、生食添加の場合のAPTT時間を2秒以内ではあるが有意に短縮させたのに対し、DHSG-HbVはどの血漿比率の場合においても生食の場合と差はみられなかった。

カリクレイン-キニン系に対する影響は、血漿にそれぞれこれら3種のHbVまたは生食を添加し、37°Cにて24時間インキュベーション後、血漿中高分子キニンノーゲンの分解による低分子化された高分子キニンノーゲンの出現をイムノブロットング法にて検出した。血漿に対し40%あるいは60%にてDPPG-HbVまたはDPPG-HbV(no PEG)を添加させた場合、intactな高分子キニンノーゲンが減少し、低分子化された高分子キニンノーゲンの増加が顕著に観察される。これに対して、DHSG-HbVではいずれの血漿比率の場合においても生食の場合と差はみられず、DHSG-HbVは血漿中高分子キニンノーゲンの分解を引き起こさないことが示された(Fig. 2)。

以上の検討から、陰性荷電のDPPGを構成成分とするHbVではPEG修飾がなければ補体の活性化が惹起されるのに対し、PEG修飾することで補体の活性化が抑えられることが明らかとなった。生理食塩水中でゼータ電位を測定するとDPPG-HbV(no PEG)が-14.5 mV、DPPG-HbVが-3.4 mVであり<sup>30)</sup>、表面荷電の影響を裏付けていた。しかしながら、ここに示したごとくDPPG-HbVでは、わずかではあるが、凝固時間、特にAPTT時間の短縮およびカリクレイン-キニン系の活性化を引き起こした。これに対し、DHSG-HbVは、補体系、APTT時間、カリクレイン-キニン系のいずれに対しても影響が無いことが示された。DHSG-HbVのゼータ電位は-2.6 mVでDPPG-

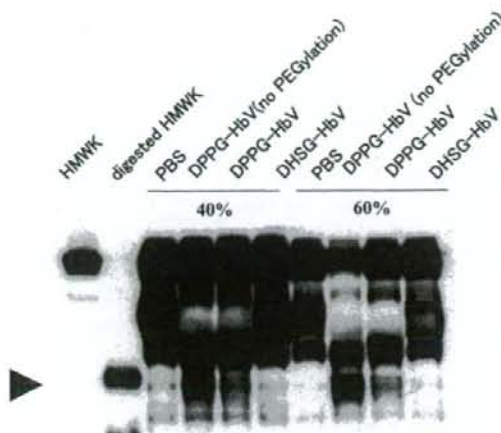


Fig. 2. Activation of kallikrein-kinin cascade by HbVs. HbVs or saline were mixed with plasma at 40% or 60% at 37 °C for 24 h. Appearance of digested S-HMWK was detected using western blot analysis as a result of kallikrein activation. Arrowhead (▶) indicates digested S-HMWK.

HbVのそれとほとんど変わらないことから、単に表面荷電だけでなく、構成脂質の親水性頭部(hydrophilic head group)が作用の有無に影響を及ぼすものと考えられる。

いずれにしても、今後の臨床試験に用いられる現行のHbVは、血漿中の補体系に影響を及ぼさないということから、“補体活性化関連偽アレルギー反応”と呼ばれるリポソーム投与直後の心血管系の急性副作用<sup>31)</sup>に対する懸念はほとんど無いと推測される。加えて、凝固系やカリクレイン-キニン系への影響も無いことは、ヒト血漿タンパクへの高い適合性を示している。

第1章の血小板に対するHbVの影響に関して、げっ歯類においては血小板上に補体成分C3bが結合するCR1レセプターを有しているが、ヒトを含む霊長類では有さないことを上述した。これに対し、ヒトを含む霊長類では赤血球がCR1レセプターを有しているため、補体活性化に伴って免疫複体の赤血球への結合が報告されている<sup>32)</sup>。そのため、補体活性化を惹起しうる化合物および医薬品のヒト血液を対象としたin vitroにおける適合試験や臨床試験においては、赤血球も相互作用する可能性のある血液構成成分の一つとして重要であり、そのため、赤血球をモニターする意義や結果の解釈にも影響する可能性を考慮しておく必要がある。しかしながら、少なくとも今後の臨床試験に用いられる現行のHbVは、in vitroの評価試験において血漿中の補体系に影響を及ぼさないため、補体成分を介してHbVが赤血球と結合する可能性は少ないと推測される。

#### おわりに

HbVが臨床応用に向けて、前臨床試験でその有効性、安全性について検討しなければならない事項の中に、免疫系および血液構成成分に対する影響があげられている。ヒト血液細胞およびヒト血漿タンパク系を用いた評価により、止血また炎症反

応にも関する血小板に対し、HbV自体による活性化作用はみられないこと、またアゴニストによる活性化を亢進するような作用はないことが示された。自然免疫に重要な働きをする好中球の機能（走化能、脱顆粒、活性酸素産生）にも影響を与えなかった。造血機能への影響としては、短期間であれば造血前駆細胞活性を損なうことはないことが示された。またリポソームの特性から補体の活性化が懸念されたが、現行のHbVでは活性化はみられず、また、凝固系、カリクレイン・キニン系にも影響はみられなかった。しかしながらin vitroでは評価できない抗体産生、投与後の補体価の変動、リンパ球の抗原刺激による増殖反応等については現在ラットを用いて検討をおこなっている。本稿にては詳細は割愛したが、それらの影響は、投与直後に一過性の抑制がみられるものの1週間では回復することをみだしている<sup>26,32)</sup>。以上のことから、免疫系、および血液構成成分に対してHbVが高い適合性を持つことを示すことができた。

最近、Natansonら<sup>34)</sup>は、ヘモグロビンを基盤とする非セル型の人工酸素運搬体を対象とした無作為化された前臨床試験および臨床試験の中から、一定の基準を満たした16トライアルにおいて、死亡のリスクが30%増、心筋梗塞のリスクが2.7倍増加しているというメタ解析の結果を報告した。この報告に伴って、ヘモグロビンを基盤とする非セル型の人工酸素運搬体の安全性を見直し、リスクの増加の原因を明らかにすべきとの指摘がなされている<sup>35)</sup>。このような状況下において、我が国だけが開発を進めているセル型の人工酸素運搬体の一つであるHbVに、大きな期待がよせられる。

## 謝辞

本研究は、厚生科学研究費補助金（高度先端医療研究事業）「酸素運搬能を有する人工赤血球の創製とその評価に関する研究（平成9年～11年）」「臨床応用可能な人工赤血球の創製に関する研究（平成12年～14年）」、厚生科学研究費補助金（高度先端医療研究事業）「人工赤血球の安全性向上に関する研究（平成15年～17年）」、「人工酸素運搬体の臨床応用に関する研究（平成18年～20年）」によって行われた。記して謝意を表す。

## 参考文献

1. Sakai H, Sou K, Horinouchi H, Kobayashi K, Tsuchida E. Haemoglobin-vesicles as artificial oxygen carriers: present situation and future visions. *J Intern Med* 2008;263:4-15.
2. 高折益彦: 人工血液としての条件. *人工血液* 2002;10:28-35.
3. Rabinovici R, Rudolph AS, Feuerstein G: Characterization of hemodynamic, hematologic, and biochemical responses to administration of liposome-encapsulated hemoglobin in the conscious, freely moving rat. *Circ Shock* 1989;29:115-32.
4. Rabinovici R, Rudolph AS, Yue T, Feuerstein G: Biological responses to administration of liposome-encapsulated hemoglobin (LEH) are improved by a PAF antagonist.

- Circ Shock* 1990;31:431-5.
5. Phillips WT, Klipper R, Fresne D, Rudolph AS, Javors M, Goins B: Platelet reactivity with liposome-encapsulated hemoglobin in the rat. *Exp Hematol* 1997;25:1347-56.
6. Reinish LW, Bally MB, Loughrey HC, Cullis PR: Interactions of liposomes and platelets. *Thromb Haemost* 1988;60:518-523.
7. Doerschuk CM, Gie RP, Bally MB, Cullis PR, Reinish L: Platelet distribution in rabbits following infusion of liposomes. *Thromb Haemost* 1989;61:392-6.
8. Loughrey HC, Bally MB, Reinish LW, Cullis PR: The binding of phosphatidylglycerol (PG) liposomes to rat platelets is mediated by complement. *Thromb Haemost* 1990;64:172-6.
9. Klinger MHF: Platelets and inflammation. *Anat Embryol* 1997;196:1-11.
10. Gawaz M, Langer H, May AE: Platelets in inflammation and atherogenesis. *J Clin Invest* 2005;115:3378-84.
11. Wakamoto S, Fujihara M, Abe H, Sakai H, Takeoka S, Tsuchida E, Ikeda H, Ikebuchi K: Effects of poly(ethylene glycol)-modified hemoglobin vesicles on agonist-induced platelet aggregation and RANTES release in vitro. *Artif Cells Blood Substit Immobil Biotechnol* 2001;29:191-201.
12. Baggiolini M, Dahinden CA: CC chemokines in allergic inflammation. *Immunol Today* 1994;15:127-33.
13. Wakamoto S, Fujihara M, Abe H, Yamaguchi M, Azuma H, Ikeda H, Takeoka S, Tsuchida E: Effects of hemoglobin vesicles on resting and agonist-stimulated human platelets in vitro. *Artif Cells Blood Substit Biotechnol* 2005;33:101-11.
14. Hagberg IA, Lyberg T: Evaluation of circulating platelet-leukocyte conjugates: a sensitive flow cytometric assay well suited for clinical studies. *Platelets* 2000;11:151-60.
15. 幸村 近, 林 由紀子, 池田久實: フローサイトメトリーを用いた活性化血小板の検出法. *臨床病理* 1999;47:447-52.
16. Hynes RO: Integrins: versatility, modulation, and signaling in cell adhesion. *Cell* 1992; 69:11-25.
17. Hatipoglu U, Gao XP, Verral S, Sejourne F, Pitrak D, Alkan-Onyuksel H, Rubinstein I: Sterically stabilized phospholipids attenuate human neutrophils chemotaxis in vitro. *Life Sci* 1998; 63:693-9.
18. Bellemare F, Israel-Assayag E, Cormier Y: PC:PS liposomes induce a recruitment of neutrophils and the release of TNF alpha in the lungs of mice sensitized with *Saccaropolyspora rectivirgula*. *Eur J Clin Invest* 1995;25:340-5.
19. Ito T, Fujihara M, Abe H, Yamaguchi M, Wakamoto S, Takeoka S, Sakai H, Tsuchida E, Ikeda H, Ikebuchi K: Effects of poly(ethylene glycol)-modified hemoglobin

- vesicles on N-formyl-methionyl-leucyl-phenylalanine-induced responses of polymorphonuclear neutrophils in vitro. *Artif Cells Blood Substit Immobil Biotechnol* 2001;29:427-37.
20. Galdiero F, Carratelli CR, Bentivoglio C, Capasso C, Cioffi S, Folgore A, Gorga F, Ianniello R, Mattera S, Nuzzo I, Rizzo A, Tufano MA: Correlation between modification of membrane phospholipids and some biological activity of lymphocytes, neutrophils and macrophages. *Immunopharmacol Immunotoxicol* 1991;13:623-42.
  21. Torchilin VP: Recent advances with liposomes as pharmaceutical carriers. *Nat Rev Drug Discov* 2005;4:145-60.
  22. Sou K, Klipper R, Goins B, Tsuchida E, Phillips WT: Circulation kinetics and organ distribution of Hb-vesicles developed as a red blood cell substitute. *J Pharmacol Exp Ther* 2005;312:702-9.
  23. Sakai H, Horinouchi H, Tomiyama K, Ikeda E, Takeoka S, Kobayashi K, Tsuchida E: Hemoglobin-vesicles as oxygen carriers: Influence on phagocytic and histopathological changes in reticuloendothelial system. *Am J Pathol* 2001;159:1079-88.
  24. Sakai H, Horinouchi H, Yamamoto M, Ikeda E, Takeoka S, Takaori M, Tsuchida E, Kobayashi K: Acute 40 percent exchange-transfusion with hemoglobin-vesicles (HbV) suspended in recombinant human serum albumin solution: degradation of HbV and erythropoiesis in a rat spleen for 2 weeks. *Transfusion* 2006;46:339-47.
  25. Ikeda T, Horinouchi H, Kohno M, Izumi Y, Watanabe M, Sakai H, Sou K, Tsuchida E, Kobayashi K: Resuscitation effect and long term effect of Hb vesicles on organ function in beagle dog. *Artif Cells Blood Substitutes Biotechnol* 2008;36:214.
  26. Abe H, Azuma H, Yamaguchi M, Fujihara M, Ikeda H, Sakai H, Takeoka S, Tsuchida E: Effects of hemoglobin vesicles, a liposomal artificial oxygen carrier, on hematological responses, complement and anaphylactic reactions in rats. *Artif Cells Blood Substit Biotechnol* 2007;35:157-72.
  27. Yamaguchi M, Fujihara M, Wakamoto S, Sakai H, Takeoka S, Tsuchida E, Azuma H, Ikeda H: Influence of hemoglobin vesicles, cellular-type artificial oxygen carriers, on human umbilical cord blood hematopoietic progenitor cells in vitro. *J Biomed Mater Res A* 2008. (in press)
  28. Bell D, Mueller SG: Enhanced stimulation of erythropoiesis. Patent EP099644, 2004.
  29. Fowler DA, Rosenthal GJ, Sommadossi JP: Effect of recombinant human hemoglobin on human bone marrow progenitor cells: protection and reversal of 3'-azido-3'-deoxythymidine-induced toxicity. *Toxicology Letters* 1996;85:55-62.
  30. Moqattash S, Lutton JD, Rosenthal G, Abu-Hijleh MF, Abraham NG: Effect of blood substitute, recombinant hematology, on in vivo hematopoietic recovery from AZT toxicity. *Acta Haematol* 1997;98:76-82.
  31. 阿部秀樹, 藤原満博, 東 寛, 池田久實. リボソームと補体. *人工血液* 2003;11:151-9.
  32. Chonn A, Cullis PR, Devine DV: The role of surface charge in the activation of the classical and alternative pathways of complement by liposomes. *J Immunol* 1991;146:4234-41.
  33. Cunningham CM, Kingzette M, Richards RL, Alving CR, Lint TF, Gewurz H: Activation of human complement by liposomes: a model for membrane activation of the alternative pathway. *J Immunol* 1979;122:1237-42.
  34. Devine DV, Wong K, Serrano K, Chonn A, Cullis PR: Liposome-complement interactions in rat serum: implications for liposome survival studies. *Biochim Biophys Acta* 1994;1191:43-51.
  35. Griep MA, Fujikawa K, Nelsestuen GL: Binding and activation properties of human factor XII, prekallikrein, and derived peptides with acidic lipid vesicles. *Biochemistry* 1985;24:4124-30.
  36. Mitropoulos KA, Martin JC, Reeves BE, Esnouf MP: The activation of the contact phase of coagulation by physiologic surfaces in plasma: the effect of large negatively charged liposomal vesicles. *Blood* 1989;73:1525-33.
  37. Alving CR, Richards RL, Guirguis AA: Cholesterol-dependent human complement activation resulting in damage to liposomal model membranes. *J Immunol* 1977;118:342-7.
  38. Alving CR: Natural antibodies against phospholipids and liposomes in humans. *Biochem Soc Trans* 1984;12:342-4.
  39. Szebeni J, Wassef NM, Rudolph AS, Alving CR: Complement activation in human serum by liposome-encapsulated hemoglobin: the role of natural anti-phospholipid antibodies. *Biochim Biophys Acta* 1996;1285:127-30.
  40. Bradley AJ, Devine DV, Ansell SM, Janzen J, Brooks DE: Inhibition of liposome-induced complement activation by incorporated poly (ethylene glycol)-lipids. *Arch Biochem Biophys* 1998;357:185-94.
  41. Klibanov AL, Maruyama K, Torchilin VP, Huang L: Amphipathic polyethyleneglycols effectively prolong the circulation time of liposomes. *FEBS Lett* 1990;268:235-7.
  42. Woodle MC, Matthey KK, Newman MS, Hidayat JE,

- Collins LR, Redemann C, Martin FJ, Papahadjopoulos D: Versatility in lipid compositions showing prolonged circulation with sterically stabilized liposomes. *Biochim Biophys Acta* 1992;1105:193-200.
43. Laverman P, Boerman OC, Oyen WJG, Corstens FHM, Storm G: In vivo applications of PEG liposomes: unexpected observations. *Crit Rev Ther Drug Carrier Syst* 2001;18:551-66.
44. Szebeni J, Baranyi L, Savay S, Bodo M, Morse DS, Basta M, Stahl GL, Bünger R, Alving CR: Liposome-induced pulmonary hypertension: properties and mechanism of a complement-mediated pseudoallergic reaction. *Am J Physiol Heart Circ Physiol* 2000;279:H1319-28.
45. Wassef NM, Johnson SH, Graeber GM, Swartz GM Jr, Schultz CL, Hailey JR, Johnson AJ, Taylor DG, Ridgway RL, Alving CR: Anaphylactoid reactions mediated by autoantibodies to cholesterol in miniature pigs. *J Immunol* 1989;143:2990-5.
46. Uziely B, Jeffers S, Isacson R, Kutsch K, Wei-Tsao D, Yehoshua Z, Libson E, Muggia FM, Gabizon A: Liposomal doxorubicin: antitumor activity and unique toxicities during two complementary phase I studies. *J Clin Oncol* 1995;13:1777-85.
47. Koukourakis MI, Koukouraki S, Giatromanolaki A, Archimandritis SC, Skarlatos J, Beroukas K, Bizakis JG, Retalis G, Karkavitsas N, Helidonis ES: Liposomal doxorubicin and conventionally fractionated radiotherapy in the treatment of locally advanced non-small-cell lung cancer and head and neck cancer. *J Clin Oncol* 1999;17:3512-21.
48. Lyass O, Uziely B, Ben-Yosef R, Tzemach D, Heshing NI, Lotem M, Brufman G, Gabizon A: Correlation of toxicity with pharmacokinetics of pegylated liposomal doxorubicin (Doxil) in metastatic breast carcinoma. *Cancer* 2000;89:1037-47.
49. Chanan-Khan A, Szebeni J, Savay S, Liebes L, Rafique NM, Alving CR, Muggia FM: Complement activation following first exposure to pegylated liposomal doxorubicin (Doxil): possible role in hypersensitivity reactions. *Ann Oncology* 2003; 14:1430-7.
50. Abe H, Fujihara M, Azuma H, Ikeda H, Ikebuchi K, Takeoka S, Tsuchida E, Harashima H: Interaction of hemoglobin vesicles, a cellular-type artificial oxygen carrier, with human plasma: effects on coagulation, kallikrein-kinin, and complement systems. *Artif Cells Blood Substit Biotechnol* 2006;34:1-10.
51. Szebeni J, Fontana JL, Wassef NM, Mongan PD, Morse DS, Dobbins DE, Stahl GL, Bunger R, Alving CR: Hemodynamic changes induced by liposomes and liposome-encapsulated hemoglobin in pigs. A model for pseudoallergic cardiopulmonary reactions to liposomes: role of complement and inhibition by soluble C1 and anti-C5a antibody. *Circulation* 1999;99:2302-2309.
52. Cornacoff JB, Hebert LA, Smead WL, VanAman ME, Birmingham DJ, Waxman FJ: Primate erythrocyte-immune complex-clearing mechanism. *J Clin Invest* 1983;71:236-47.
53. 阿部秀樹, 山口美樹, 藤原満博, 酒井宏水, 武岡真司, 土田英俊, 東 寛, 池田久實: ヘモグロビン小胞体 (HbV) 投与がラット免疫系に及ぼす影響. *人工血液* 2004;12:55.
54. Natanson C, Kern SJ, Lurie P, Banks SM, Wolfe AM: Cell-free hemoglobin-based blood substitutes and risk of myocardial infarction and death: a meta-analysis. *JAMA* 2008; 299:304-12.
55. Furgusson DA, McIntyre L: The future of clinical trials evaluating blood substitutes. *JAMA* 2008;99:2324-6.

# Artificial Oxygen Carriers, Hemoglobin Vesicles and Albumin–Hemes, Based on Bioconjugate Chemistry

Eishun Tsuchida,\*<sup>†</sup> Keitaro Sou,<sup>†</sup> Akito Nakagawa,<sup>†</sup> Hiromi Sakai,<sup>†</sup> Teruyuki Komatsu,<sup>†,‡</sup> and Koichi Kobayashi<sup>§</sup>

Research Institute for Science and Engineering, Waseda University, Tokyo 169-8555, Japan, PRESTO, Japan Science and Technology Agency (JST), and Department of General Thoracic Surgery, School of Medicine, Keio University, Tokyo 160-8582, Japan. Received October 10, 2008; Revised Manuscript Received December 10, 2008

Hemoglobin (Hb, Mw: 64 500) and albumin (Mw: 66 500) are major protein components in our circulatory system. On the basis of bioconjugate chemistry of these proteins, we have synthesized artificial O<sub>2</sub> carriers of two types, which will be useful as transfusion alternatives in clinical situations. Along with sufficient O<sub>2</sub> transporting capability, they show no pathogen, no blood type antigen, biocompatibility, stability, capability for long-term storage, and prompt degradation in vivo. Herein, we present the latest results from our research on these artificial O<sub>2</sub> carriers, Hb-vesicles (HbV) and albumin–hemes. (i) HbV is a cellular type Hb-based O<sub>2</sub> carrier. Phospholipid vesicles (liposomes, 250 nm diameter) encapsulate highly purified and concentrated human Hb (35 g/dL) to mimic the red blood cell (RBC) structure and eliminate side effects of molecular Hb such as vasoconstriction. The particle surface is modified with PEG-conjugated phospholipids, thereby improving blood compatibility and dispersion stability. Manipulation of physicochemical parameters of HbV, such as O<sub>2</sub> binding affinity and suspension rheology, supports the use of HbV for versatile medical applications. (ii) Human serum albumin (HSA) incorporates synthetic Fe<sup>2+</sup>porphyrin (FeP) to yield unique albumin-based O<sub>2</sub> carriers. Changing the chemical structure of incorporated FeP controls O<sub>2</sub> binding parameters. In fact, PEG-modified HSA-FeP showed good blood compatibility and O<sub>2</sub> transport in vivo. Furthermore, the genetically engineered heme pocket in HSA can confer O<sub>2</sub> binding ability to the incorporated natural Fe<sup>2+</sup>protoporphyrin IX (heme). The O<sub>2</sub> binding affinity of the recombinant HSA (rHSA)-heme is adjusted to a similar value to that of RBC through optimization of the amino acid residues around the coordinated O<sub>2</sub>.

## 1. INTRODUCTION

Transfusion of donor blood is currently an indispensable routine procedure in modern medical treatments because the risk of transmission of viral illness has become extremely low. Nevertheless, this level of safety has been achieved at great cost and hepatitis virus or unknown pathogens cannot be excluded completely, even by the nucleic acid amplification test (NAT) system. Furthermore, the transfusion of donor blood necessitates cross matching and compatibility tests to avoid a hemolytic reaction in the recipient, and the donated red blood cells (RBCs) must be refrigerated at 4 °C (up to 3 weeks in Japan). These requirements limit the availability of blood transfusion in disaster or emergency situations.

During the past several decades, various artificial O<sub>2</sub> carriers have been synthesized and studied for as RBC substitutes by many scientists in the fields of organic chemistry, inorganic chemistry, biochemistry, and polymer chemistry. These O<sub>2</sub> carriers are classified as perfluorocarbon-based materials, synthetic Fe<sup>2+</sup>porphyrin-based materials, and Hb-based materials. In this review, we highlight recent developments of our research related to RBC substitutes of the latter two types.

Actually, Hb consists of four polypeptide chains (globin proteins), each of which has an Fe<sup>2+</sup>protoporphyrin IX (heme) as a prosthetic group. The globin chain forms a compact globular conformation; the heme group is incorporated into the hydrophobic pocket with an axial coordination of histidine (1). On

exposure of the Hb solution to O<sub>2</sub>, the heme forms a stable O<sub>2</sub> adduct complex. However, if the heme is eliminated from the globin wrapping, the heme complex is oxidized immediately and irreversibly to its Fe<sup>3+</sup> state by proton-driven oxidation or  $\mu$ -oxo dimer formation (2). In the 1970s and 1980s, much research was directed to mimic the O<sub>2</sub> carrier by synthesizing substituted porphyrin derivatives. In aprotic solvents, the proton-driven oxidation is excluded completely. Therefore, the remaining problem is how to suppress irreversible oxidation via dimerization. One successful approach was steric modification of porphyrin. Some superstructured Fe<sup>2+</sup>porphyrins were prepared using an elegant organic synthesis technique (2–4). In particular, Collman reported that the tetrakis( $\alpha,\alpha,\alpha,\alpha$ -*p*-ivalamido)phenylporphyrinatoiron complex with 1-methylimidazole can reversibly bind O<sub>2</sub> in benzene at room temperature (5, 6). Nevertheless, these synthetic porphyrins were all oxidized irreversibly in aqueous media.

To create a hydrophobic environment in water, it is possible to use a bilayer membrane of a phospholipid vesicle instead of globin protein. In 1983, we synthesized an amphiphilic Fe<sup>2+</sup>porphyrin having four alkylphosphocholine groups (lipid-heme), which is efficiently embedded into the bilayer of the phospholipid vesicle to yield a homogeneous hybrid. This lipidheme/phospholipid vesicle can bind and release O<sub>2</sub> under physiological conditions (Figure 1) (7–9). The 10 mM lipid-heme/phospholipid vesicle solution dissolves 29 mL O<sub>2</sub>/dL compared to 27 mL/dL of human blood. Subsequent to that finding, we synthesized over 60 lipidheme molecules. A new lipidheme having four dialkyl-*sn*-glycerophosphocholine groups is self-organized in water to form self-assembled porphyrin bilayer vesicles without phospholipid (10). Furthermore, in 1995, we found that synthetic Fe<sup>2+</sup> porphyrin bearing a covalently linked proximal base (FeP1) is incorporated into human serum

\* To whom correspondence should be addressed. Eishun Tsuchida, Ph.D. Phone: +81-3-5286-3120. Fax: +81-3-3205-4740. E-mail: eishun@waseda.jp.

<sup>†</sup> Waseda University.

<sup>‡</sup> JST.

<sup>§</sup> Keio University.

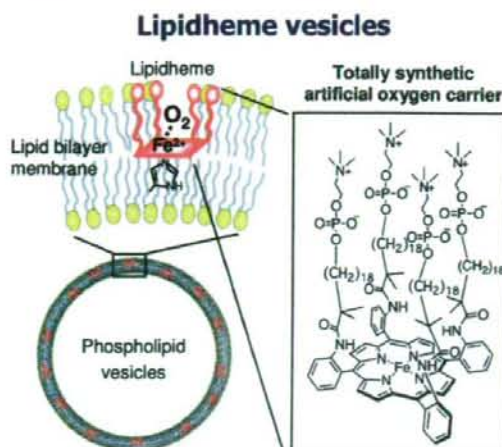


**Figure 1.** Lipidheme phospholipid vesicles as a totally synthetic artificial  $O_2$  carrier (7).

albumin (HSA) and the obtained HSA-FePI hybrid coordinates  $O_2$  in aqueous medium (11).

In 1985, we began the study of Hb-based  $O_2$  carriers using purified human Hb aiming at the beneficial utilization of outdated RBC to support the present blood donation-transfusion system. This project has been supported for a long time by Japanese Red Cross Society and Ministry of Health and Welfare, Japan. On the basis of a fundamental concept that the cellular structure of RBC is necessary for  $O_2$  transport in the bloodstream, we designed the phospholipid vesicle encapsulating Hb: the so-called Hb-vesicle. It has to be emphasized that the Hb-vesicle comprises a concentrated Hb solution and four kinds of natural and synthetic lipids that assemble to form a hierarchical corpuscle structure (molecular assembly) through the well-regulated secondary interactions, such as hydrophobic and electrostatic interactions. To date, chemically modified Hb of several types have been developed as RBC substitutes or  $O_2$  therapeutic reagents. Herein, we review the latest developments of our research into Hb-vesicles and albumin-hemes.

## 2. HEMOGLOBIN VESICLES THAT MIMIC THE RBC CELLULAR STRUCTURE

### 2.1. Physiological Importance of Cellular Structure of RBC for Encapsulated Hb Design.

Historically, stroma-free Hb isolated from RBCs were tested as a principal material for carrying  $O_2$ . However, the plasma retention time of stroma-free Hb is particularly short (half-life of 0.5–1.5 h) because of the dissociation of the Hb tetramer ( $\alpha_2\beta_2$ ; Mw, 64 500; 6.5 nm diameter) into dimers ( $2\alpha\beta$ ), which are subsequently filtered by the kidney (12). Cell-free Hb-based  $O_2$  carriers have been developed to overcome the problems of stroma-free Hb through chemical modification, "bioconjugation", of Hb molecules (Figure 2). They include intramolecularly cross-linked Hb (DCLHb) to prevent dimerization, recombinant cross-linked Hb produced by *E. coli*, polymerized Hb using glutaraldehyde or other cross-linkers, and polymer-conjugated Hb such as PEG-conjugated Hb and polysaccharide-conjugated Hb (13–21). During the long history of the development of cell-free Hb-based  $O_2$  carriers (HBOCs), the many side effects of stroma-free Hb and chemically modified Hbs have been well-documented: renal toxicity; entrapment of gaseous messenger molecules (NO and CO) inducing vasoconstriction, hypertension, reduced blood flow, and reduced tissue oxygenation at microcirculatory levels (22–25); neurological disturbances; malfunction of esophageal motor function (18); myocardial

lesions (26, 27); and death (28). These side effects of Hb molecules underscore the importance of the large dimension of HBOCs or the RBC cellular structure. Retrospective and recent observations have indicated the main justifications for Hb encapsulation in RBCs: (i) a decreased high colloidal osmotic pressure (15); (ii) prevention of the removal of Hb from blood circulation; (iii) prevention of direct contact of toxic Hb molecules and the endothelial lining (29); (iv) retardation of reactions with endogenous NO and CO (24, 25, 30, 31) (Figure 3); (v) preservation of the chemical environment in cells, such as the concentration of phosphates (2,3-DPG, ATP, etc.) and other electrolytes; (vi) RBCs are the major component that renders blood as non-Newtonian and viscous, which is necessary to pressurize the peripheral artery for homogeneous blood distribution and for maintenance of blood circulation (32); (vii) the RBC cellular structure retards  $O_2$ -release in comparison to acellular Hb solutions (33, 34), thereby retaining  $O_2$  to peripheral tissues where  $O_2$  is required. For those reasons, the optimal structure of Hb-based  $O_2$  carriers might be to mimic the RBC cellular structure.

In 1957, Chang performed the pioneering work of Hb encapsulation to mimic the cellular structure of RBCs (35); microcapsules (5  $\mu\text{m}$ ) were prepared using nylon, collodion, and other materials. Toyoda in 1965 (36) and the Kambara–Kimoto group in 1968 (37) also investigated encapsulation of Hbs with gelatin, gum arabic, silicone, and so forth. Nevertheless, results emphasized the extreme difficulty of regulating the particle size to be appropriate for blood flow in the capillaries and to obtain sufficient biocompatibility. After Bangham and Horne reported in 1964 (38) that phospholipids assemble to form vesicles in an aqueous medium and encapsulated water-soluble materials in their inner aqueous interior (39), it seemed reasonable to use such vesicles for Hb encapsulation. Djordjevic and Miller in 1977 (40) prepared liposome-encapsulated Hb (LEH) composed of phospholipids, cholesterol, fatty acids, and so forth. The US Naval Research Laboratories and collaborators demonstrated remarkable progress in the use of LEH (41–43). Terumo Corp. (Tokyo) developed different LEH, so-called Neo Red Cells (44, 45) (Table 1).

However, some intrinsic issues of encapsulated Hbs remained, which were related mainly to the nature of molecular assembly and particle dispersion. What we call Hb-vesicles (HbV), with their high-efficiency production processes and improved properties, were established by our group based on technologies of molecular assembly in concert with precise analyses of their pharmacological and physiological aspects (46–48) (Tables 2 and 3). We use stable carbonylhemoglobin (HbCO) for purification with pasteurization at 60 °C for 10 h. The purity of the obtained Hb solution is extremely high (49, 50). Use of the stable and purified HbCO enables concentration of the Hb solution to more than 40 g/dL using ultrafiltration and easy handling of Hb encapsulation using the extrusion method, without causing Hb denaturation. It has been confirmed that HbV encapsulates nearly 35 g/dL within a thin bilayer membrane. In final processing, CO of HbCO in HbV is photodissociated by irradiation of visible light under an  $O_2$  atmosphere, and it converts to HbO<sub>2</sub> (51).

In fact, Hb autoxidizes to form metHb and loses its  $O_2$ -binding ability during storage and during blood circulation (52–56). For that reason, metHb formation must be prevented. A method exists to preserve deoxygenated Hbs in a liquid state from using intrinsic characteristics of Hb: the Hb oxidation rate in a solution is dependent on the  $O_2$  partial pressure; moreover, deoxyHb is not autoxidized at ambient temperatures (56). In the case of HbV, not only the encapsulated Hb but also the capsular structure (liposome) must be physically stabilized to prevent

## Hemoglobin-based O<sub>2</sub> carriers

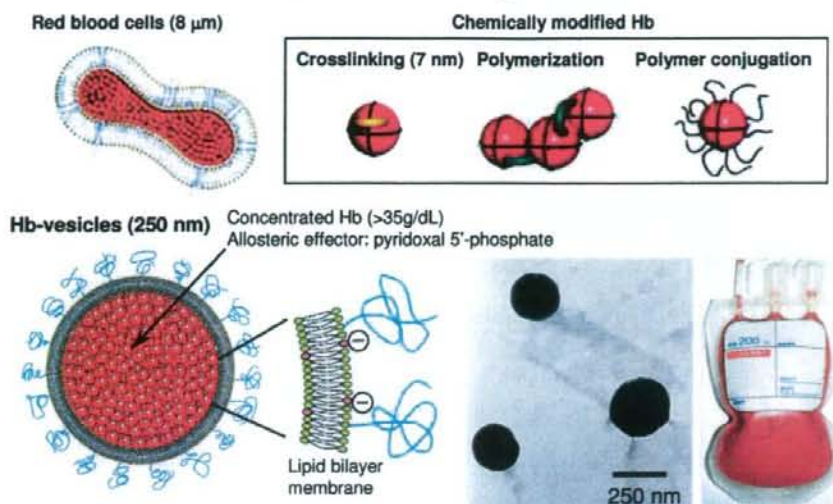


**Figure 2.** Schematic representation of a series of Hb-based O<sub>2</sub> carriers. Cross-linked Hb, polymerized Hb, and polymer-conjugated Hb are based on the chemical modification of Hb molecules (chemically modified Hbs). In the case of Hb-vesicles, a purified and concentrated Hb solution (35 g/dL) is encapsulated in phospholipid vesicles and the surface is modified using PEG chains. The particle size is well-regulated at 250 nm.

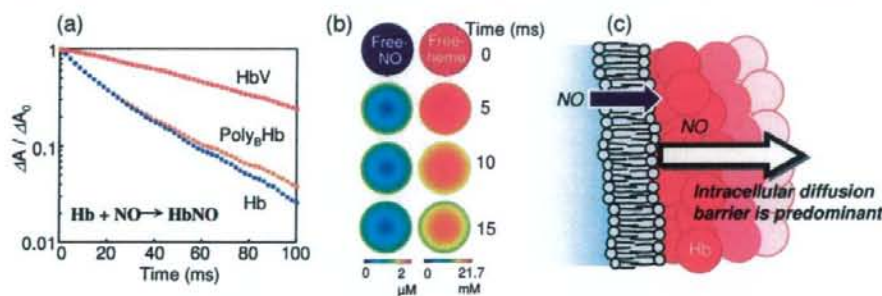


**Figure 3.** Encapsulation of Hb in vesicles retards NO binding. (a) Time courses of NO binding with HbV, human Hb with PLP (Hb/PLP = 1:2.5 by mol), and polymerized bovine Hb (Poly<sub>6</sub>Hb) observed by stopped-flow rapid scan spectrophotometry. The level of reaction was plotted on a semilogarithmic graph as a ratio of absorption at 430 nm ( $\Delta A$ ) at time  $t$ , to the initial absorption ( $\Delta A_0$ ) at time 0. NO-bubbled PBS ([NO] = 3.8  $\mu$ M) and deoxygenated-Hb-containing solutions in PBS ([heme] = 3.0  $\mu$ M) were mixed (31). (b) Schematic two-dimensional representation of the simulated time courses of distributions of unbound free NO and unbound free heme in one HbV (250 nm). Both free NO and unbound hemes are distributed heterogeneously. The concentration changes gradually from the surface to the core, indicating formation of the intracellular diffusion barrier (30). (c) The phospholipid bilayer membrane cannot have any barrier function to gas diffusion. The determinant factor of retardation of NO-binding should be the intracellular diffusion barrier, which was induced by (i) intrinsically larger binding rate constant of NO to a heme in an Hb molecule, (ii) numerous hemes as sites of gas entrapment at a higher Hb concentration, (iii) a slowed gas diffusion in the intracellular viscous Hb solution, and (iv) a longer gas diffusion distance in a larger capsule.

irreversible intervesicular aggregation, fusion, and leakage of the encapsulated Hb.

In addition to HbV, new encapsulated Hbs without liposomes have emerged with the use of recent advanced nanotechnologies, such as polymersome (57) and PEG-poly( $\epsilon$ -caprolactone) copolymer nanoparticles (58). In vivo evaluation of O<sub>2</sub>-carrying capacities of these new materials is anticipated. Encapsulation of Hb can reduce the toxicity of cell-free Hbs. However, numerous hurdles must be surmounted to realize encapsulated Hbs because of the components of the capsules themselves and their structural complexity as a molecular assembly. It is also important to consider the larger dosage requirement of encapsulated Hb for blood substitution than those of conventional drug delivery systems, which require no large dosage.

**2.2. Structural Stabilization and Destabilization using Polymerization or PEG Conjugation.** Liposomes, as molecular assemblies, have generally been characterized as structurally

unstable. The US Naval Research Laboratory tested the addition of cryoprotectants and lyoprotectants such as trehalose to LEH for its preservation as a powder without causing hemolysis after rehydration (59, 60). In addition, many researchers have developed stabilization methods for liposomes that use polymer chains (61–64). Polymerization of phospholipids that contain two dienyl groups (1,2-dioctadecadienyl-*sn*-glycero-3-phosphatidylcholine; DODPC) was studied extensively by our group. For example, gamma-ray irradiation induces radiolysis of water molecules and generates OH radicals that initiate intermolecular polymerization of dienyl groups in DODPC. This method produces remarkably stable liposomes, resembling rubber balls, which are resistant to freeze–thawing, freeze–drying, and rehydration (65, 66). Actually, the polymerized liposomes were so stable that they were not degraded easily in the macrophages, even 30 days after injection (67). It became widely believed that polymerized lipids are inappropriate for intravenous injec-



**Table 1. List of Representative Liposome-Encapsulated Hbs (LEH) Extensively Studied Aiming at Industrialization and Other Potential Encapsulated Hbs Using Biodegradable Polymers**

product name	group	characteristics	current status
Hb vesicles (HbV)	Waseda Univ. and Keio Univ.	1. Pasteurization of HbCO at 60 °C for virus inactivation 2. Lipid composition to improve blood compatibility 3. PEG modification and deoxygenation for 2 yr storage 4. [Hb] = 10 g/dL	preclinical
Neo Red Cells (NRC)	Terumo Corp.	1. Inositol hexaphosphate to regulate $P_{50}$ (= 40–50 Torr) 2. Lipids: HSPC/cholesterol/fatty acid/PEG-lipid 3. Storage in a refrigerator for 6 months 4. [Hb] = 6 g/dL	preclinical
artificial red cells (ARC)	NOF Corp. and Waseda Univ.	1. Polymerized lipids (DODPC) for stabilization 2. Storage in powdered or frozen state 3. Difficulty in degradation in RES	suspended
liposome-encapsulated Hb (LEH)	US Naval Research Laboratory	1. Freeze-dried powder with trehalose 2. Low Hb encapsulation efficiency 3. Thrombocytopenia, complement activation	suspended
synthetic erythrocytes	Rush-Presbyterian-St. Luke's Medical Center, Univ. Illinois	1. The first attempt of LEH	suspended
Hb-loaded particles (HbP)	East China Univ. of Science and Technology	1. Hb encapsulation by poly( $\epsilon$ -caprolactone) (PCL) and poly( $\epsilon$ -caprolactone-ethylene glycol) (PCL-PEG) 2. Double emulsion and solvent diffusion/evaporation method 3. Biodegradable	basic study
polymersome-encapsulated Hb (PEH)	The Ohio State Univ.	1. Self-assembly of amphiphilic diblock copolymers composed of poly(ethylene oxide) (PEO), poly(caprolactone) (PCL), and poly(lactide) (PLA) 2. Biodegradable and biocompatible	basic study

**Table 2. Physicochemical Characteristics of Hb Vesicles**

parameter	
particle diameter	250–280 nm
$P_{50}$ (O <sub>2</sub> ) <sup>a</sup>	25–28 Torr
[Hb]	10 g/dL
[heme]	6.2 mM
[metHb]	<3%
[HbCO]	<2%
suspending medium	physiologic saline solution (0.9% NaCl)
colloid osmotic pressure	0 Torr
intracellular Hb concentration	ca. 35 g/dL
lipid composition	DPPC/cholesterol/DHSG/ DSPE-PEG <sub>5000</sub>
$\zeta$ potential <sup>b</sup>	-18.7 mV
weight ratio of Hb to lipids	1.6–1.9 (w/w)
viscosity <sup>c</sup>	3.8 cP
lamellarity	nearly 1
stability for storage at room temperature	>2 years, purged with N <sub>2</sub>
circulation half-life	35 h (rats)

<sup>a</sup> Measured with a Hemox Analyzer (pH 7.4, 37 °C). <sup>b</sup> Measured with a Zeta-Sizer Nano ZS ([NaCl] = 20 mM, pH 7.4). <sup>c</sup> Measured with Anton Parr Rheometer M301 (268 s<sup>-1</sup>, 25 °C).

**Table 3. Characteristics of Hb-Vesicles As a Transfusion Alternative**

- Human derived Hb solution is purified rigorously by pasteurization and ultrafiltration. The blood type antigens and pathogens are eliminated for utmost safety.
- Encapsulation of concentrated Hb solution (>35 g/dL), like RBCs.
- Small particle size (250 nm) for homogeneous distribution in the plasma phase of circulating blood.
- Shielding of the side effects of molecular Hbs by the lipid membrane.
- PEG modification for dispersion stability for long-term storage and in the bloodstream.
- Surface properties of HbV (PEG, negative charge, etc.) for blood compatibility.
- Prompt degradation and excretion of the components after entrapment in RES.
- Sufficient oxygen transporting capacity ([Hb] = 10 g/dL, cf, [Hb] of blood = 12–15 g/dL).
- Physicochemical properties are easily adjustable because of the nature of the "molecular assembly".

tion because of the difficulty in excretion. Subsequently, it was clarified that selection of appropriate lipids (phospholipid/cholesterol/negatively charged lipid/PEG-conjugated phospholipid) and that their composition is important to enhance the

stability of nonpolymerized liposomes (45, 68). Surface modification of liposomes with PEG-conjugated lipids is sufficient for dispersion stability (69). In fact, in comparison to RBCs, HbV is highly resistant to hypotonic shock, freeze–thawing, and enzymatic attack by phospholipase A<sub>2</sub> (70).

We investigated the possibility of long-term preservation of HbV during storage for two years through a combination of deoxygenation and PEG modification (71). As little as 0.3 mol % PEG-conjugated lipid stabilizes the dispersion state and prevents aggregation and fusion for two years through steric hindrance (71–73). The original metHb content (ca. 3%) before preservation decreased gradually to less than 1% after 1 month because of the presence of a reductant, such as homocysteine, inside the vesicles that consumed the residual O<sub>2</sub> and gradually reduced the trace amount of metHb. The rate of metHb formation was strongly dependent on the O<sub>2</sub> partial pressure: a lack of increase in the metHb formation was observed because of the intrinsic stability of the deoxygenated Hb. In fact, the metHb content did not increase for two years. These results suggest the possibility that the HbV suspension can be stored at room temperature for at least two years, which would enable stockpiling of HbV for any emergency.

**2.3. Vesicular Surface Modification with PEG and Negative Charges for Blood Compatibility.** Liposome is not a solute: it is a particle in a suspension. The particle surface might be recognized, leading to interaction with blood components including complements. The so-called *injection reaction*, or pseudoallergy, results from complement activation, giving rise to anaphylatoxins, which trigger various hypersensitivity reactions. This reaction is observed sometimes not only with liposomal products (74), but also with fat emulsions (75), and a perfluorocarbon emulsion (76). Therefore, examination of blood compatibility of encapsulated Hbs is important for clinical use. Transient thrombocytopenia and pulmonary hypertension in relation to complement activation is an extremely important hematologic effect observed in rodent models after infusion of LEH (containing DPPG: 1,2-dipalmitoyl-*sn*-glycero-3-phosphatidylglycerol) developed by the US Naval Research Laboratory (77, 78) and other products. In our group, exchange transfusion of prototype HbV (containing DPPG, no PEG modification) in anesthetized rats engendered transient thrombocytopenia and slight hypertension (79). Similar effects were also observed for administration of negatively charged liposomes

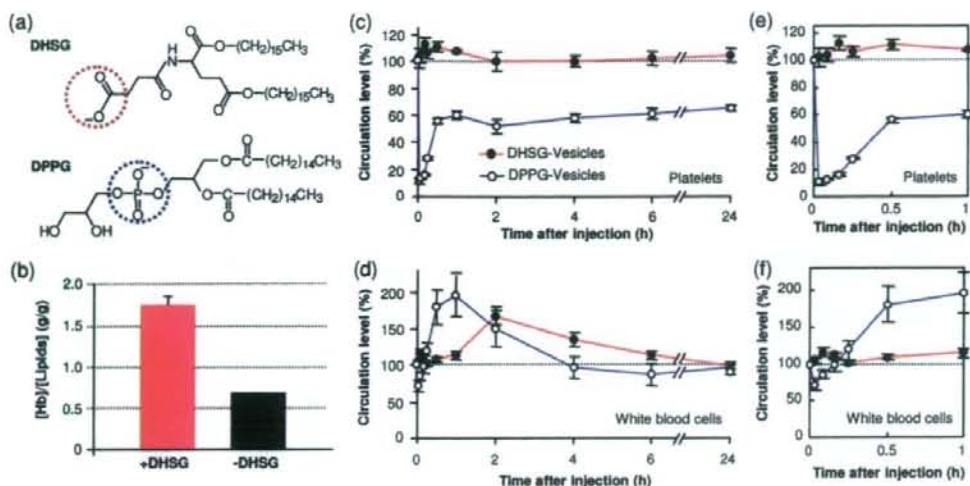


**Figure 4.** Effect of negatively charged vesicles on encapsulation capability and blood compatibility of HbV. (a) Chemical structures of negatively charged lipids, 1,5-*O*-dihexadecyl-*N*-succinyl-L-glutamate (DHSG) and 1,2-dipalmitoyl-*sn*-glycero-phosphatidylglycerol (DPPG). (b) Effect of DHSG on encapsulation efficiency of Hb (35 g/dL). (c–f) Circulation levels of platelets (c) and white blood cells (d) after intravenous infusion of vesicles containing 9 mol % DHSG (DHSG-vesicles) or 9 mol % DPPG (DPPG-vesicles) in rats (lipids; 280 mg/kg body weight). The right side graphs show the initial fluctuations in platelets (e) and white blood cells (f).

(80, 81). The transient reduction in platelet counts caused by complement-bound liposomes was also associated with sequestration of platelets in the lung and liver. Such nonphysiological platelet activation probably engenders initiation and modulation of inflammatory responses because platelets contain several potent proinflammatory substances. A negatively charged lipid is required for encapsulating a large amount of Hb using a minimum amount of lipids (46–48). Therefore, we had to overcome the problem of conventional negatively charged vesicles to achieve blood compatibility. In the present formation of HbV, we use a negatively charged lipid (DHSG; 1,5-*O*-dihexadecyl-*N*-succinyl-L-glutamate) and confirmed the considerable improvement of Hb encapsulation efficiency (Figure 4a,b). It must be emphasized that the present vesicle formulation for HbV apparently does not induce thrombocytopenia or complement activation in animal experiments (Figure 4c–f) (82, 83), probably because the present HbV contains PEG-modification and a different type of negatively charged lipid (DHSG), not DPPG or a fatty acid.

Ikeda and his co-workers (83–86) thoroughly examined blood compatibility of HbV to human blood *in vitro*. The present PEG-modified HbV containing DHSG did not affect the extrinsic or intrinsic coagulation activities of human plasma, although HbV containing DPPG and no PEG modification tended to shorten the intrinsic coagulation time. The kallikrein-kinin cascade of the plasma was activated slightly by the prototype DPPG-HbV, but not by the present PEG-DHSG-HbV. The exposure of human platelets to high concentrations of the present HbV (up to 40%) *in vitro* did not cause platelet activation and did not adversely affect the formation and secretion of prothrombotic substances or proinflammatory substances that are triggered by platelet agonists. These results imply that HbV, at concentrations of up to 40%, has aberrant interactions with neither unstimulated nor agonist-induced platelets. It can be concluded that the present PEG-DHSG-HbV has higher blood compatibility.

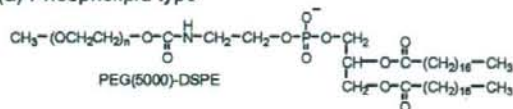
For surface modification of HbV with PEG chains, several PEG-conjugated lipids having amino acid backbone have been synthesized, as presented in Figure 5b,c (87, 88). For other applications, these PEG-conjugated lipids are available to modify the surfaces of not only HbV but also lipid vesicles. Because the PEG-lipids having a large hydrophilic group form thermo-

dynamically unstable self-assemblies, called micelles (73), they easily dissociate to monomers and spontaneously incorporate only to the outer surface of preformed HbV, as illustrated in Figure 5d (45, 72). Using this method, the required amount of PEG-conjugated lipid can be reduced by half or less because only the outer surface of HbV requires PEG chains. In addition, the PEG chains extending from the inner surface are expected to reduce the interior volume for encapsulation because of their exclusion volume effect. Therefore, modification only to the outer surface is important to encapsulate large amounts of Hb in lipid vesicles. To immobilize the hydrophilic macromolecules stably, such as PEG chains and proteins on lipid vesicles, a large hydrophobic anchor having a tetraacyl structure has been synthesized (Figure 5c,e). It has been confirmed that this hydrophobic anchor can stably immobilize PEG chains of high molecular weight (Mw 12 500) or water-soluble proteins (87, 89). These surface modification technologies and lipid chemistry have been applied to the development of other functional biomaterials (87–93).

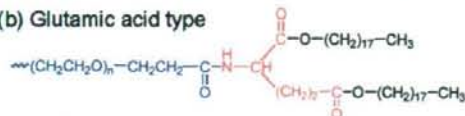
**2.4. Circulation Time, Biodistribution, and Metabolism.** The dosage of blood substitutes is expected to be considerably larger than those of other drugs, while their circulation time is considerably shorter than that of RBCs. Therefore, their biodistribution, metabolism, excretion, and side effects must be characterized in detail, especially in relation to the reticuloendothelial system (RES, alternatively, the mononuclear phagocytic system, MPS). Normally, free Hb released from RBCs is bound rapidly to haptoglobin and is consequently removed from circulation by hepatocytes. However, when the Hb concentration is greater than the haptoglobin binding capacity, unbound Hb is filtered through the kidney, where it is actively absorbed. Hemoglobinuria and eventual renal failure occur when the kidney reabsorption capacity is exceeded. The encapsulation of Hb in vesicles completely suppresses renal excretion. However, HbV in the bloodstream is ultimately captured by phagocytes in the RES in much the same manner as senescent RBCs are, as confirmed by radioisotope  $^{99m}\text{Tc}$ -labeled HbV injection (42, 94). The circulation half-life is dose-dependent: for the dosage of 14 mL/kg body weight, the circulation half-life was 34.8 h in rats and 62.6 h in rabbits (Figure 6a). The HbV are finally distributed mainly in the liver,

## Poly(ethylene glycol)-conjugated lipids

## (a) Phospholipid type



## (b) Glutamic acid type



## (c) Lysine type

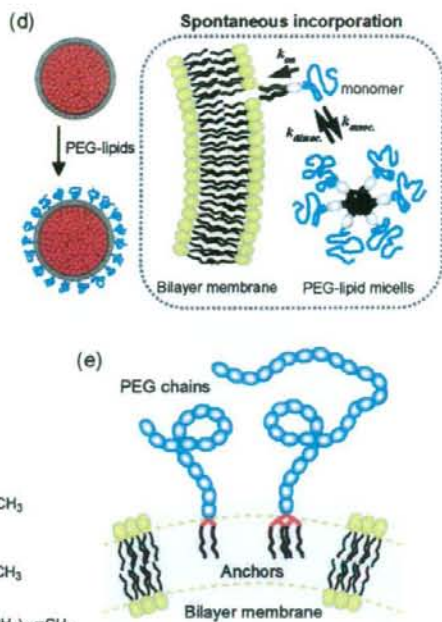
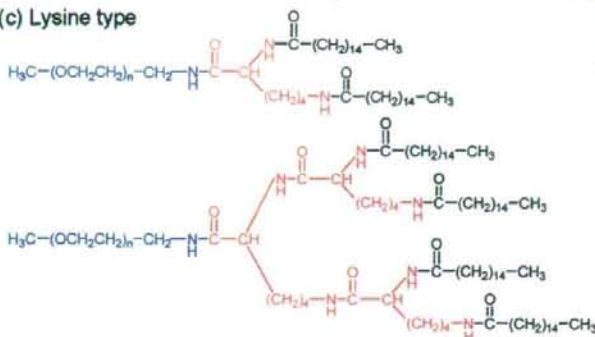


**Figure 5.** Surface modification of HbV with PEG chains. (a–c) Chemical structures of PEG-conjugated lipids. (a) PEG(5000)-DSPE is commercially available and widely used for surface modification of lipid vesicles. (b) Glutamic acid-type and (c) lysine-type PEG-conjugated lipids were reported previously (87, 88). (d) PEG-modification of the HbV using the spontaneous incorporation of a PEG-lipid into the bilayer membrane (72). (e) Immobilization of the large water-soluble polymers on the bilayer membranes (87, 89).

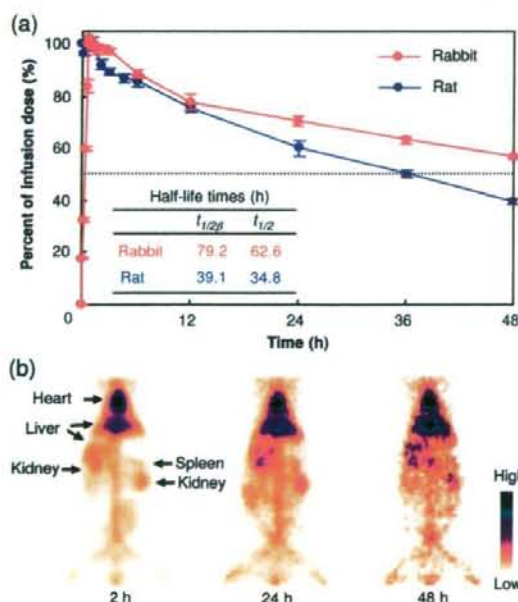


**Figure 6.** Circulation kinetics and organ distribution of HbV labeled with technetium-99m after top-loading intravenous infusion (14 mL/kg) in rats and rabbits (94). (a) Elimination profiles of HbV from blood. (b) Static gamma camera images of a rabbit acquired at 2, 24, and 48 h after HbV infusion.

spleen, and bone marrow (Figure 6b). The species-dependent circulation time is inferred to be dependent upon the species-specific weight balance of phagocyte organs, particularly the liver, spleen, and bone marrow, against body weight (94). The

circulation half-life in the case of the human body can be estimated as about 2–3 days at the same dosage.

It is generally accepted that the liposome clearance by RES at a small dosage is accelerated by opsonization (absorption of plasma proteins such as antibodies and complements on the liposomal surface). In fact, PEG-modification prevents opsonization for prolonged circulation times (95). However, considering a condition in which the dosage of HbV is extremely high and requires a considerable amount of opsonins, and in which HbV does not induce complementary activation (82, 83), then opsonin-dependent phagocytosis would not be a major component in the case of HbV with a large dosage. Actually, opsonin-independent phagocytosis, a direct recognition by macrophages, has been clarified in some studies (96, 97).

Analysis of the spleen by transmission electron microscopy (TEM) 1 day after infusion of HbV revealed the presence of HbV particles in the phagosomes of macrophages (98) (Figure 7). However, after 7 days, the HbV structure cannot be observed. We confirmed transient splenomegaly with no irreversible damage to the organs and complete metabolism within a week. The phagocytic activity transiently, but not completely, decreased 1 day after injection, and it turned to increasing at 3 days. The influence on the defense function and its mechanism has been carefully examined in the ongoing research. Immunohistochemical staining with a polyclonal anti-human Hb antibody was used as the marker of Hb in the HbV. Results clarified that HbV had almost disappeared in both the spleen and liver after 7 days.

Bilirubin and iron are believed to be released during metabolism of Hb, but our animal experiments of topload infusion, daily repeated infusions, and 40% blood exchange showed that neither of those products increased in the plasma within 14 days (99–101). Bilirubin would normally be excreted in the bile as a normal pathway; no obstruction or stasis of the bile is expected to occur in the biliary tree. Berlin blue staining

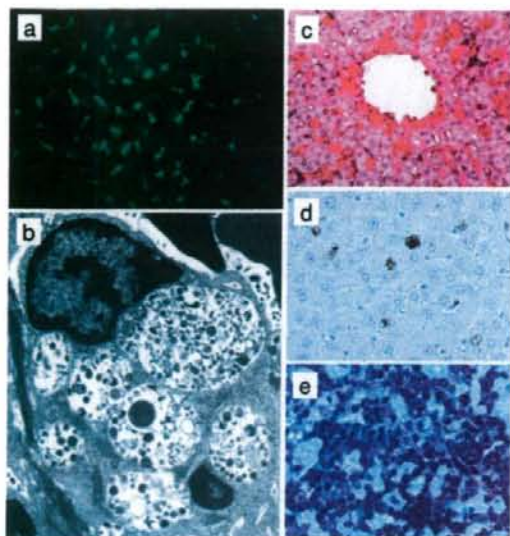


**Figure 7.** Histopathological examination of livers and spleens of rodents after injection of HbV. (a) Hamster liver 1 h after injection of fluorescence-labeled HbV, observed by a confocal laser scanning microscopy. The strong fluorescence indicates that HbV particles accumulate in Kupffer cells. (b) TEM of rat spleen macrophage 1 day after injection of HbV. The small black dots are HbV particles in phagosomes. The particles disappeared within a week (data not shown) (98). (c) Rat liver 1 day after injection of HbV. It was immunohistochemically stained with anti-human Hb antibody. The red parts indicate the presence of Hb in HbV. It disappeared within a week (data not shown) (98). (d) Rat liver 7 day after injection of HbV. It was immunohistochemically stained with anti-methoxy-PEG antibody. The brown parts indicate the presence of PEG derived from PEG-lipid of HbV during the degradation. Fourteen days after injection, PEG was not detectable (data not shown) (102). (e) Rat spleen 3 days after 40% exchange transfusion with HbV. It was stained with Giemsa method. A large amount of blue cells, erythroblasts, are seen, indicating the enhanced hematopoiesis for the complete recovery of hematocrit within one week, while HbV are degraded in RES (101).

revealed considerable deposition of hemosiderin in the liver and spleen, even after 14 days. Moderate splenomegaly and hemosiderin deposition were also confirmed in the spleen after injection of stored RBCs, partly because of the accumulation and degradation of stored RBCs with lowered membrane deformability and shortened circulation half-life (101).

As for membrane components of Hb-vesicles, the plasma cholesterol level elevated transiently 3 days after injection: cholesterol was released from macrophages after degradation of HbV in phagosomes (99, 101). It was recently clarified using  $^3\text{H}$ -cholesterol that cholesterol of HbV is released from macrophages to blood; it is ultimately excreted in feces. The PEG chain is widely used for surface modification of liposomal products. The chemical cross-linker succinic acid ester of PEG-conjugated phospholipid is susceptible to hydrolysis to release PEG chains during metabolism. Actually, immunohistochemistry using an anti-methoxy-PEG antibody clarified that PEG had disappeared from the liver and spleen in one week (102). The released PEG chains, which are known as inert macromolecules, are expected to be excreted in urine through the kidneys (103).

To determine the physiological capacity of RES for degradation of HbV, we tested massive intravenous doses by daily repeated infusion of 10 mL/kg body weight/day into Wistar rats for 14 days. The cumulative dosage was 140 mL/kg body weight (Hb and lipids, 20 689 mg/kg body weight). The total volume was equal to 2.5 times the total blood volume (56 mL/kg body weight) (100). Although splenohepatomegaly was considerable,

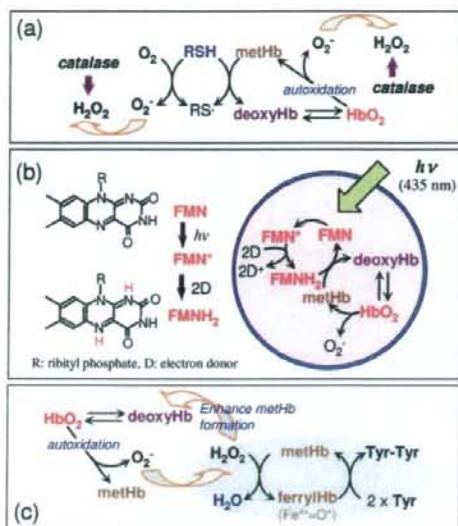


**Figure 8.** Artificial methHb reduction systems in HbV. (a) Coencapsulation of thiols (RSH), such as glutathione and homocysteine, reduces methHb. However, thiols react with  $\text{O}_2$  to generate  $\text{O}_2^-$  and  $\text{H}_2\text{O}_2$ . A more reactive thiol such as cysteine shows extremely rapid reaction with  $\text{O}_2$  and adversely facilitates metHb formation. Coencapsulation of catalase effectively eliminates  $\text{H}_2\text{O}_2$  and prevent such reactions (52, 53, 56). (b) Photoreduction system by coencapsulation of flavin mononucleotide (FMN) and an electron donor such as EDTA and methionine. Visible light irradiation (435 nm) primarily converts FMN to the photoexcited triplet  $\text{FMN}^*$ , and this reacts with two electron donors (D) to generate  $\text{FMNH}_2$ . MetHb is rapidly reduced once  $\text{FMNH}_2$  is produced (54). (c) During autoxidation of Hb and in blood circulation,  $\text{H}_2\text{O}_2$  is a potent methHb enhancer. A combination of L-tyrosine (Tyr) and methHb effectively eliminates  $\text{H}_2\text{O}_2$  and prolongs the functional lifetime of HbV (55).

all rats tolerated the infusions; their body weight increased during the succeeding 14 days until their intended sacrifice. The phagocytosed HbV had disappeared, though the considerable hemosiderin deposition was confirmed in the spleen, liver, kidney, adrenal gland, and bone marrow. We were unable to define a lethal dose of HbV in this experiment.

The profile of liposome clearance is species-dependent. More precise data are necessary to extrapolate the phenomena observed in animal experiments to humans. However, these results imply that the metabolism of HbV and excretion are within the physiological capacity that has been well-characterized for the metabolism of senescent RBCs and conventional liposomal products.

**2.5. Regulation of  $\text{O}_2$  Transporting Capability (MetHb Reduction,  $\text{P}_{50}(\text{O}_2)$ ).** Actually, Hb encapsulation provides a unique opportunity to add new functions to particles by coencapsulation or embedding of functional molecules (52–56, 104–106). MetHb formation of HbV during the preservation is completely prevented simply by deoxygenation. However, autoxidation of  $\text{HbO}_2$  is initiated once HbV is administered into the bloodstream because the entire methHb enzymatic system is eliminated during the Hb purification for the utmost safety from infection. An artificial methHb reducing system is required to prolong the  $\text{O}_2$ -carrying capacity of HbV. We have tested coencapsulation of reductants to directly reduce methHb and a photoreduction system using a photosensitizer such as flavin mononucleotide (FMN). A more practical method is to create an artificial enzymatic system using L-tyrosine (Tyr) and methHb that eliminates  $\text{H}_2\text{O}_2$  as does catalase (Figure 8).

Without a chemical modification of Hb,  $\text{O}_2$  binding affinity (expressed as  $\text{P}_{50}(\text{O}_2)$ ,  $\text{O}_2$  tension at which Hb is half-saturated

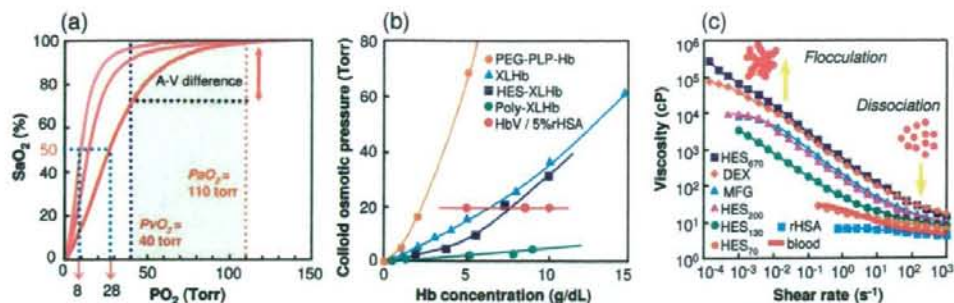


**Figure 9.** Regulation of physicochemical properties of HbV for versatile applications. (a) Oxygen dissociation curves of HbVs. Oxygen affinity ( $P_{50}$ , partial pressure of oxygen at which Hb is half-saturated with oxygen) is regulated by coencapsulation of PLP (105, 106). (b) Colloid osmotic pressure (COP) of chemically modified Hb solutions increase with the Hb concentration (15). In contrast, HbV particles have no oncotic effect. The figure shows 20 Torr when HbV is suspended in 5% rHSA. XLHb, intramolecularly cross-linked Hb. (c) Rheological properties of HbV suspended in various plasma substitute solutions (22). [Hb] = 10 g/dL, 25 °C.

with  $O_2$ ) of HbV can be regulated by coencapsulation of an allosteric effector (105, 106) (Figure 9a). The  $P_{50}(O_2)$  of purified Hb in a saline solution (in the presence of  $Cl^-$ ) is about 14 Torr; Hb strongly binds  $O_2$  and does not release  $O_2$  at 40 Torr (partial pressure of mixed venous blood). Historically, it has been regarded that the  $O_2$  affinity is expected to be regulated similarly to that of RBC, namely, about 25–30 Torr, using an allosteric effector or by a direct chemical modification of the Hb molecules. This enables sufficient  $O_2$  unloading during blood microcirculation, as evaluated by the arterio-venous difference in the levels of  $O_2$  saturation in accordance with an  $O_2$  equilibrium curve. Pyridoxal 5'-phosphate (PLP) is coencapsulated in HbV as an allosteric effector to regulate  $P_{50}(O_2)$  (105, 106). The main binding site of PLP is the N-terminal of the  $\alpha$ -chain and  $\beta$ -chain and  $\beta$ -82 Lysine within the  $\beta$ -cleft, which is part of the binding site of the natural allosteric effector, 2,3-diphosphoglyceric acid (2,3-DPG). The bound PLP retards the dissociation of the ionic linkage between the  $\beta$ -chains of Hb during conversion of deoxy to oxyHb in the same manner as 2,3-DPG does. Therefore, the  $O_2$  affinity of Hb decreases in the presence of PLP. The  $P_{50}(O_2)$  of HbV can be regulated to 8–150 Torr by coencapsulating the appropriate amount of PLP or inositol hexaphosphate as an allosteric effector. Equimolar PLP to Hb (PLP/Hb = 1/1 by mol) was coencapsulated, and  $P_{50}(O_2)$  was regulated to 18 Torr. Furthermore,  $P_{50}(O_2)$  was regulated to 32 Torr when the molar ratio PLP/Hb was 3/1. The  $O_2$  affinities of HbV can be regulated easily without changing other physical parameters, whereas in the case of the other modified Hb solutions, their chemical structures determine their  $O_2$  binding affinities. Consequently, regulation is difficult. The present HbV contains PLP at PLP/Hb = 2.5 by mol; the resulting  $P_{50}(O_2)$  is about 25–28 Torr, which shows sufficient  $O_2$  transporting capacity as a transfusion alternative. Actually, HbV has been shown to provide  $O_2$ -transport capacity that is both sufficient and comparable to that of RBCs in experiments related to extreme blood exchange (68, 69, 79, 105, 107, 108) and fluid resuscitation from hemorrhagic shock (102, 109–112) (Figure 10). A recent experiment of HbV as a priming solution for cardiopulmonary bypass (CPB) in a rat model showed that HbV protects neurocognitive function by transporting  $O_2$  to brain tissue even when the hematocrit is reduced markedly (113).

The appropriate  $O_2$  binding affinities for  $O_2$  carriers have not yet been decided completely. However, the easy regulation of the  $O_2$  binding affinity might be useful to meet the requirement of clinical indications such as oxygenation of ischemic tissues. The  $P_{50}(O_2)$  of HbV without PLP and  $Cl^-$  is 8–9 Torr. This formulation is effective for targeted  $O_2$  delivery to anoxic tissues caused by reduced blood flow (107, 114, 115).

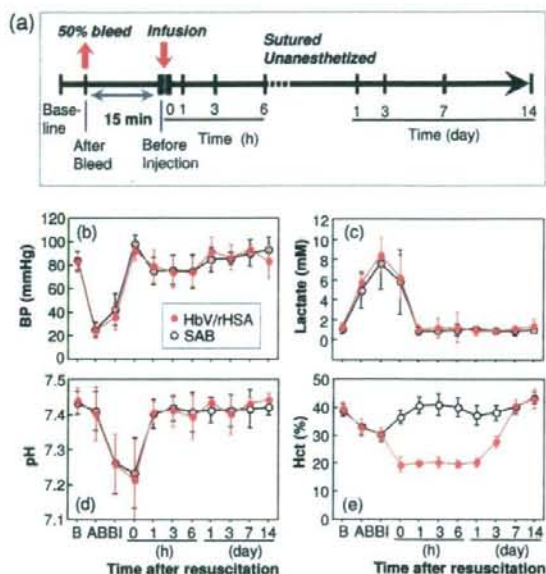


**Figure 10.** (a) Scheme depicting the experimental protocol of hemorrhagic shock and resuscitation (102). Shock was induced by withdrawing 50% of circulating blood volume from Wistar rats. After 15 min, they were resuscitated with either HbV suspended in recombinant human serum albumin (HbV/rHSA) or shed autologous blood (SAB). (b) blood pressure, (c) lactate, (d) pH, and (e) hematocrit (Hct). Mean  $\pm$  SD. B, Baseline; AB, after bleeding; BI, before injection (B-6 h,  $n = 24$ ; 1–14 days,  $n = 5$ ).

**2.6. Rheological Properties and Their Physiological Implications for Tissue Oxygenation.** The extremely high concentration of the HbV suspension ([Hb] = 10 g/dL; [lipids] = 6 g/dL, volume fraction, ca. 40 vol %) imparts an  $O_2$  carrying capacity that is comparable to that of blood. The HbV suspension does not possess a colloid osmotic pressure (COP), because one HbV particle (ca. 250 nm diameter) contains about 30 000 Hb molecules. In fact, HbV acts as a particle, not as a solute. Therefore, HbV must be suspended in or conjoined with an aqueous solution of a plasma substitutes. This requirement is identical to that for emulsified perfluorocarbon, which does not possess COP (116, 117); it contrasts to characteristics of other Hb-based  $O_2$  carriers, intramolecular cross-linked Hbs, polymerized Hbs, and polymer-conjugated Hbs, which all possess very high COP as protein solutions (15, 118) (Figure 9b).

**Table 4. Publications of Preclinical Studies Aiming at Applications of Hb-Vesicles for a Transfusion Alternative and for Oxygen Therapeutics**

indication	ref
1. Resuscitative fluid for hemorrhagic shock	102, 109–112
2. Hemodilution	68, 69, 79, 101, 105, 107, 108
3. Priming fluid for extracorporeal membrane oxygenator (ECMO) for cardiopulmonary bypass	113
4. Perfusate for resected organs (transplantation)	24, 129
5. Oxygenation of ischemic brain (stroke)	130
6. Oxygenation of ischemic skin flap (plastic surgery)	115, 127, 128
7. Tumor oxygenation for sensitization to irradiation	131
8. CO carrier for cytoprotection at reperfusion	132

Animal tests of HbV suspended in plasma-derived HSA or rHSA showed an O<sub>2</sub> transporting capacity that is comparable to that of blood (110, 113). We reported previously that HbV suspended in plasma-derived HSA or rHSA was almost Newtonian: no aggregation was detected microscopically (68, 69). In Japan, rHSA was very recently approved for clinical use, in May 2008 (119), but various plasma substitutes are used worldwide, such as hydroxyethyl starch (HES), dextran (DEX), and modified fluid gelatin (MFG). The selection among these plasma substitutes is best determined not only according to their safety and efficacy, but also according to their associated price, experience of clinicians, and customs of respective countries. Water-soluble polymers generally interact with particles such as polystyrene beads, liposomes, and RBCs to induce aggregation or flocculation (120, 121). For that reason, it is important to determine the compatibility of HbV with these plasma substitutes. With that background, we studied rheological properties of HbV suspended in these plasma substitute solutions using a complex rheometer and a microchannel array (122). The rheological property of an Hb-based O<sub>2</sub> carrier is important because the infusion amount is expected to be considerably large, which might affect the blood viscosity and hemodynamics.

The HbV suspended in rHSA was nearly Newtonian (Figure 9c). Its viscosity was similar to that of blood, and the mixtures with RBCs at various mixing ratios showed viscosities of 3–4 cP. Other polymers, HES, DEX, and MFG, induced flocculation of HbV, possibly by depletion interaction, and rendered the suspensions as non-Newtonian with the *shear-thinning* profile (122). These HbV suspensions showed high viscosity and a high storage modulus ( $G'$ ) because of the presence of flocculated HbV. On the other hand, HbV suspended in rHSA exhibited a very low  $G'$ . The viscosities of HbV suspended in DEX, MFG, and high-molecular-weight HES solutions responded quickly to rapid step changes of shear rates of 0.1–100 s<sup>-1</sup> and a return to 0.1 s<sup>-1</sup>, indicating that flocculation formation is both rapid and reversible. Microscopically, the flow pattern of the flocculated HbV perfused through microchannels (4.5 μm deep, 7 μm wide, 20 cmH<sub>2</sub>O applied pressure) showed no plugging. Furthermore, the time required for passage was directly related to the viscosity.

It has been regarded that lower blood viscosity after hemodilution is effective for tissue perfusion. However, microcirculatory observation shows that, in some cases, lower “plasma viscosity” decreases shear stress on the vascular wall, causing vasoconstriction and reducing the functional capillary density (123). Therefore, an appropriate viscosity might exist, which maintains the normal tissue perfusion level. The large molecular dimension of HbV can result in a transfusion fluid with high viscosity. A large molecular dimension is also effective to reduce vascular permeability and to minimize the reaction with NO and CO as vasorelaxation factors (24, 25, 30, 31)

**Figure 11.** Crystal structure of HSA with myristate (PDB ID: 1BJ5) from ref (136).

(see Figure 3). These new concepts suggest reconsideration of the design of artificial O<sub>2</sub> carriers (124). Actually, new products are appearing, although they are in the preclinical stage, not only HbV but also zero-link polymerized Hb (125) and others with larger molecular dimensions and higher O<sub>2</sub> affinities (126). Erni et al. clarified that HbV with a high O<sub>2</sub> binding affinity (low  $P_{50}(O_2)$ ), such as 8–15 Torr and high viscosity (such as 11 cP) suspended in a high-molecular-weight HES solution was effective for oxygenation of an ischemic skin flap (115, 127, 128). That study showed that HbV retains O<sub>2</sub> in the upper arterioles, then perfuses through collateral arteries and delivers O<sub>2</sub> to the targeted ischemic tissues, a concept of targeted O<sub>2</sub> delivery by an Hb-based O<sub>2</sub> carrier (114). A high O<sub>2</sub> binding affinity (low  $P_{50}(O_2)$ ) would also be effective to improve the O<sub>2</sub> saturation of Hb in pulmonary capillaries when exposed to a hypoxic atmosphere or with an impaired lung function. Some plasma substitutes cause flocculation of HbV and hyperviscosity. However, reports show that hyperviscosity would not necessarily be deteriorative and might be, in some cases, advantageous in the body (32). HbV provides a unique opportunity to manipulate the suspension rheology,  $P_{50}(O_2)$ , and other physicochemical properties, not only as a transfusion alternative, but also for other clinical applications such as oxygenation of ischemic tissues and ex vivo perfusion systems (129–132) (Table 4).

### 3. ALBUMIN-HEMES AS O<sub>2</sub> CARRYING PLASMA PROTEINS

**3.1. HSA Incorporating Synthetic Fe<sup>2+</sup> Porphyrin (HSA-FeP).** HSA (Mw: 66 500) has a remarkable ability to bind a wide variety of exogenous compounds in the human circulatory system (133). This carrier protein comprises 3 homologue helical domains (I–III) with 9 loops formed by 17 disulfide linkages; each domain contains 2 subdomains (A and B) (Figure 11) (134–137). It is known that many common drugs such as warfarin, diazepam, and ibuprofen bind to one of the two primary sites (site 1 in subdomain IIA, site 2 in subdomain IIIA) (138). In fact, HSA helps to solubilize these compounds to achieve high concentration in the bloodstream; otherwise, they would easily aggregate and be poorly distributed.

In 1995, we found that tetrakis(*o*-pivalamido)phenylporphyrinatoiron bearing a covalently linked proximal imidazole (FeP1, Figure 12) was incorporated into HSA, yielding a red HSA-FeP1 hybrid (11). This synthetic hemoprotein can reversibly bind and release O<sub>2</sub> under physiological conditions (pH 7.4, 37 °C) in much the same way as Hb. The HSA host adsorbs a maximal eight FeP1 molecules. Their stepwise binding constants ( $K_1$ – $K_8$ ) range from  $1.2 \times 10^6$  to  $1.2 \times 10^4$  (M<sup>-1</sup>) (Table

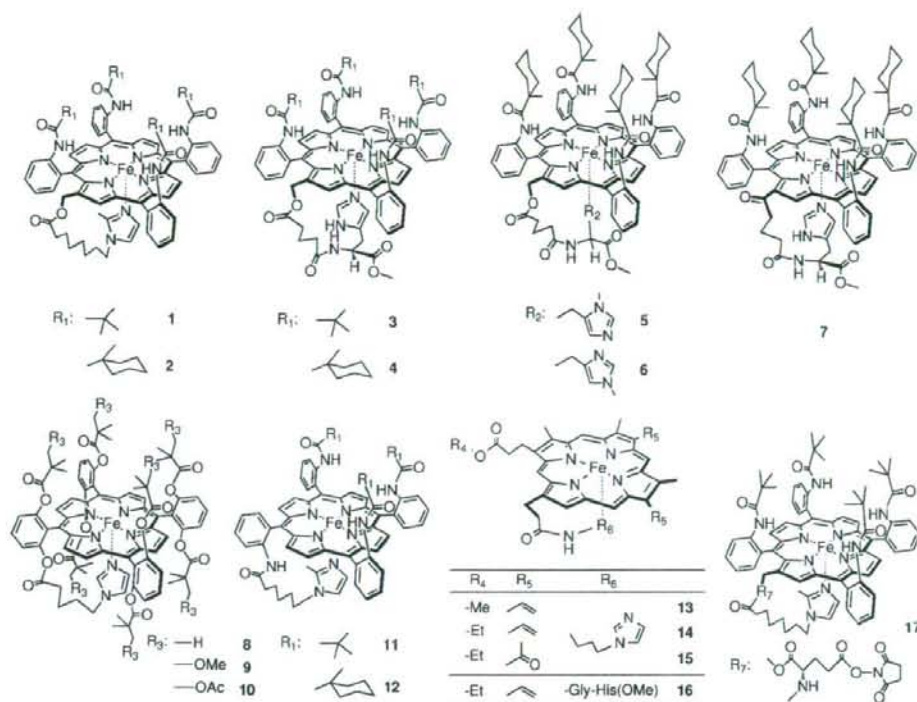


Figure 12. Structure of FePs in HSA-FePs.

3) (139, 140). Solution properties of the HSA-FeP1 solution ( $[r\text{HSA}] = 5 \text{ wt } \%$ ,  $\text{FeP}/\text{HSA} = 1\text{--}8$ , mol/mol) are almost identical to those of HSA itself: the specific gravity, 1.013; viscosity, 1.1 cP; and COP, 20 Torr. Circular dichroism (CD) spectroscopy and isoelectric focusing measurement revealed that the second-order structure and surface charge distribution of HSA were unaltered after binding of FeP1. The obtained solution showed a long shelf-life of over two years at room temperature (141). Furthermore, HSA-FeP1 has no effect on the morphology of blood cell components (142) and does not engender immunological reaction and platelet activation (143). Upon addition of  $\text{O}_2$  gas through this solution, the visible absorption spectrum immediately changed to that of the  $\text{O}_2$  adduct complex. After exposure to CO gas, a stable carbonyl complex of HSA-FeP1 was formed (139, 140). The coordination structure of FeP1 and spin-state of the central ferrous ion was characterized by IR, resonance Raman, and magnetic circular dichroism (MCD) spectroscopy (139, 140, 144). The carbonyl HSA-FeP1 moved to the NO adduct complex after bubbling NO gas (145). Subsequent ESR spectroscopy revealed that FeP1 in albumin formed a six-coordinate nitrosyl complex. The proximal imidazole moiety does not dissociate from the central ferrous ion when NO binds to the trans side (146).

The  $P_{50}(\text{O}_2)$  value of HSA-FeP1 is always constant (33 Torr,  $37^\circ\text{C}$ ) independent of the binding number of FeP1 (eq 1, Table 5)

$$\text{HSA-FeP} + \text{L} \xrightleftharpoons[k_{\text{off}}(\text{L})]{k_{\text{on}}(\text{L})} \text{HSA-FeP(L)} \quad [\text{L}: \text{O}_2 \text{ or CO}]$$

$$K(\text{L}) = [P_{50}(\text{L})]^{-1} = k_{\text{on}}(\text{L})/k_{\text{off}}(\text{L}) \quad (1)$$

The  $\text{O}_2$  binding equilibrium curve shows no cooperativity. However, the  $\text{O}_2$  transporting efficiency between the lungs [ $P(\text{O}_2)$ : ca. 110 Torr] and muscle tissue [ $P(\text{O}_2)$ : ca. 40 Torr] is 22%, which is identical to that for RBC.

Table 5. Solution Properties and Characteristics of HSA-FeP1

binding number of FeP1 ( $n$ )	1–8
binding constant of FeP1	$1.2 \times 10^6 - 1.2 \times 10^4 \text{ M}^{-1}$
$M_w$	$(66.5 + 1.3n) \text{ kDa}$
pI	4.8
viscosity <sup>a,b</sup>	1.1 cP
COP <sup>a,b,c</sup>	20 Torr
shelf life <sup>a,d</sup>	> 2 years

<sup>a</sup> In phosphate buffered solution (pH 7.3), [HSA]: 5 g/dL. <sup>b</sup> At  $37^\circ\text{C}$ .  
<sup>c</sup> A membrane filter with a cutoff ( $M_w$ ,  $30 \times 10^3$ ) was used. <sup>d</sup> At  $25^\circ\text{C}$ .

The  $\text{O}_2$  association and dissociation rate constants [ $k_{\text{on}}(\text{O}_2)$  and  $k_{\text{off}}(\text{O}_2)$ ] can be measured using laser flash photolysis (147, 148). Interestingly, the rebinding process of  $\text{O}_2$  to HSA-FeP1 included two phases (fast and slow phase), perhaps because of the different environment around each FeP1 in the protein (149). The  $P_{50}(\text{O}_2)$  value can be controlled by tuning the chemical structure of FeP1. We have synthesized quantities of Fe(II)porphyrins (Figure 12) and evaluated the  $\text{O}_2$  binding parameters of their HSA-FeP hybrids (Table 6).

Actually, FeP2 has a bulky 1-methylcyclohexanamide group on the porphyrin ring plane (150). The  $\text{O}_2$  binding affinity of HSA-FeP2 [ $P_{50}(\text{O}_2)$ : 35 Torr] was almost identical to that of HSA-FeP1. However, the stability of the oxygenated complex increased to 4.5 times its usual value [half-life  $\tau_{1/2}(\text{O}_2)$ , 9 h; pH 7.3;  $37^\circ\text{C}$ ] (150).

In general, the basicity and structure of the proximal base greatly influences the  $\text{O}_2$  binding property of  $\text{Fe}^{2+}$ porphyrin. Both FeP3 and FeP4, similar analogues having an His ligand, showed high  $\text{O}_2$  binding affinities [ $P_{50}(\text{O}_2)$ : 3 Torr] (Figure 13, Table 6). Kinetically, substitution of the 2-methylimidazole to His reduces the  $\text{O}_2$  dissociation rate constant (150). Although one might think that high  $\text{O}_2$  binding affinity is not useful as a blood substitute, it can be efficient for oxygenation of hypoxic

Table 6. O<sub>2</sub> Binding Properties of HSA-FePs in Phosphate Buffered Solution (pH 7.3, 25 °C)

FeP	$k_{on}(O_2)$ ( $\mu M^{-1} s^{-1}$ )		$k_{off}(O_2)$ ( $ms^{-1}$ )		$P_{50}(O_2)^a$ (Torr)	refs
	fast	slow	fast	slow		
1	34	9.5	0.75	0.20	13 (33)	139, 149, 150
2	46	7.3	0.98	0.16	13 (35)	150
3	36	6.1	0.059	0.010	1 (3)	150
4	54	8.8	0.089	0.014	1 (3)	150
5	54	6.8	0.02	0.0024	0.2 (1)	151
6	54	8.1	0.62	0.093	7 (22)	151
7	34	4.5	0.045	0.0059	0.8 (2)	152
8	11	1.5	0.50	0.069	28	153
9	11	2.0	0.41	0.076	23	153
10	8.9	2.3	0.34	0.088	23	153
12	29	4.4	1.10	0.16	22 (45)	154
13	—	—	—	—	0.1	155, 156
14	—	—	—	—	0.1	155, 156
15	—	—	—	—	0.4	156
16	—	—	—	—	0.1	155, 156
17	28	—	0.33	—	9 (27)	157

<sup>a</sup> At 37 °C in parentheses.

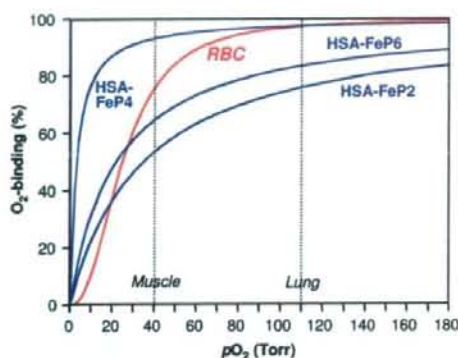


Figure 13. O<sub>2</sub> binding equilibrium curve of HSA-FePs under physiological conditions (pH 7.3, 37 °C).

regions in tumors. Furthermore, the HSA-FeP4 showed long  $\tau_{1/2}(O_2)$  of 25 h (37 °C), which is 13-fold longer than that of HSA-FeP1.

Another HSA-FeP5, in which the active porphyrin has 3-methyl-L-histidine as a proximal base, exhibits an extraordinarily high O<sub>2</sub> binding affinity [ $P_{50}(O_2)$ : 1 Torr] that approaches those of relaxed-state Hb and Mb (151). It is remarkable that replacement of the 3-methyl-L-histidine moiety by 1-methyl-L-histidine isomer (HSA-FeP6) reduced O<sub>2</sub> binding affinity to 1/35th of its former level. The low O<sub>2</sub> affinity of FeP6 is predominantly reflected by the high  $k_{off}(O_2)$  value. The axial Fe–N(1-methyl-L-histidine) coordination might be restrained by steric interaction between the 4-methylene group of the His ring and the porphyrin plane (151).

The proximal histidyl side chain can be introduced easily into the  $\beta$ -pyrrolic position of the porphyrin via an acyl bond in two steps, FeP7 (152). Although an electron-withdrawing acyl group is bound at the porphyrin periphery, the O<sub>2</sub> binding affinity of HSA-FeP7 is slightly higher than that of HSA-FeP4. The rigid His-Gly(carboxy)butanoyl spacer of FeP7 probably produces a favorable geometry to fix the imidazole onto the central Fe<sup>2+</sup> of the porphyrin.

Double-sided porphyrins (FeP8, FeP9, and FeP10) were also incorporated into HSA (153). We expected that steric encumbrances on both sides of the porphyrin enable the HSA-FePs to form a stable O<sub>2</sub> adduct complex. Actually, the  $\tau_{1/2}(O_2)$  of HSA-FeP8 was 5 h, which is 2.5-fold longer than that of HSA-FeP1. In addition, HSA-FeP8 showed high stability against hydrogen

peroxide. The HSA incorporating double-sided porphyrins would be useful for the synthetic analogue of the oxidation enzyme.

Tailed porphyrins having an  $\alpha,\alpha,\alpha,\beta$ -conformer, FeP11 and FeP12, were synthesized easily via four steps from atropisomers of tetrakis(*o*-aminophenyl)porphyrin relative to eight steps of FeP1 (154). Although HSA-FeP12 binds O<sub>2</sub> reversibly, HSA-FeP11 was quickly oxidized by O<sub>2</sub>. We concluded that the 1-methylcyclohexanamide groups are necessary for the tailed porphyrin to form an O<sub>2</sub> adduct complex under physiological conditions.

Investigations have also revealed that heme [Fe<sup>2+</sup> protoporphyrin IX; protoheme] derivatives having a proximal base at the propionate side chain (FeP13–FeP16) were incorporated into HSA (155, 156). The oxidation process of HSA-FeP13(O<sub>2</sub>) to the inactive ferric state obeyed first-order kinetics, suggesting that the  $\mu$ -oxo dimer formation was prevented by the immobilization of FeP13 into albumin. In fact, HSA-FeP15 showed lower O<sub>2</sub> binding affinity [high  $P_{50}(O_2)$ ] than the others did. The acetyl groups at the 3,8-positions of FeP15 decrease the electron density of the porphyrin macrocycle, thereby reducing the O<sub>2</sub> binding affinity. Actually, HSA-FeP16, in which the His-Gly tail coordinates to the Fe<sup>2+</sup> center, showed the most stable O<sub>2</sub> adduct complexes [ $\tau_{1/2}(O_2)$ , 90 min; pH 7.3; 25 °C] of any of these heme compounds.

**3.2. Surface-Modified HSA-FeP with PEG.** A remaining defect of HSA-FeP is that the active Fe<sup>2+</sup> porphyrin sites dissociate slowly from HSA when infused into animals because FeP is bound noncovalently to albumin. One possible solution is to bind the FeP molecule covalently to the protein. We have synthesized FeP17 having a succinimide side chain; it can react with the Lys amino group of HSA (157). The O<sub>2</sub> binding property of HSA-FeP17 is almost identical to that of HSA-FeP1.

Another approach is surface modification with PEG. Actually, PEG decollations of proteins and liposomes are well-known to enhance their plasma half-life, thermostability, nonimmunogenicity, and solubility in organic solvents (158–163). We surmised that surface modification of HSA-FeP2 by PEG might help to prolong the circulation lifetime of FeP2 and retain its O<sub>2</sub> transporting ability in vivo for a long period. Consequently, HSA-FeP2 (FeP2/HSA = 4/1, mol/mol) was modified with maleimide-PEG, and the solution properties, O<sub>2</sub> binding behavior, and circulatory persistence of the PEG-modified HSA-FeP2 [PEG(HSA-FeP2)] were examined (164). A thiolation reagent, iminothiolane, first reacted with the Lys amino groups of HSA to create active thiols that bind to  $\alpha$ -maleimide- $\omega$ -methoxy PEG (Figure 14a). Mass spectroscopy measurements and quantification of the mercapto group of PEG(HSA-FeP2)



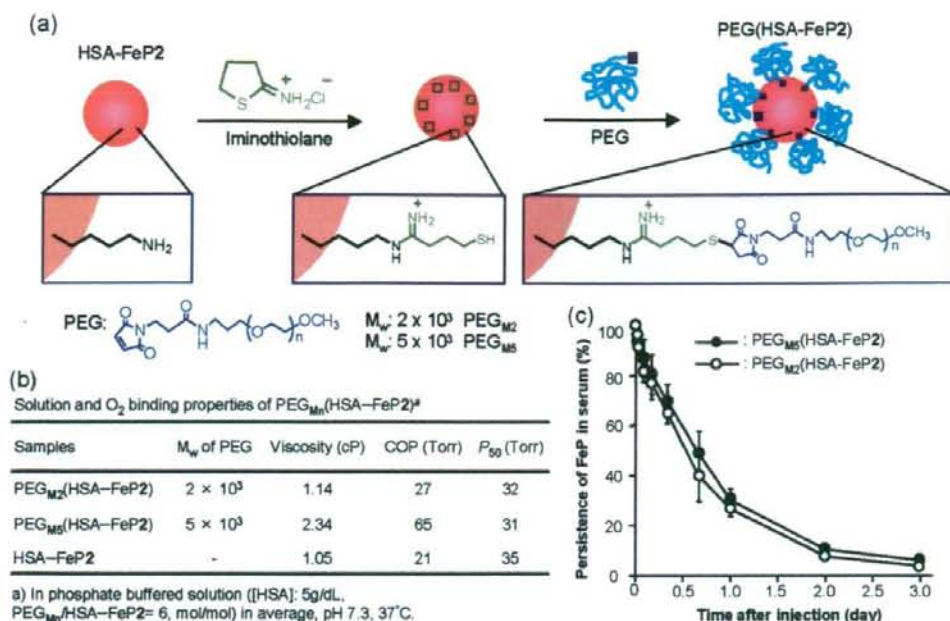


**Figure 14.** Surface modification of HSA-FeP with poly(ethylene glycol). (a) Synthetic scheme of PEG<sub>Mn</sub>(HSA-FeP2). (b) Solution and O<sub>2</sub> binding properties. (c) Persistence of FeP2 in serum after administration of PEG<sub>Mn</sub>(HSA-FeP2) into Wistar rats. Each value represents the mean ± SD of four rats.

revealed the conjugation of six PEG chains on the HSA-FeP2 surface. The initial FeP2/HSA ratio 4/1 (mol/mol) was unchanged after the PEG binding. The adjustment of viscosity is important to design an artificial O<sub>2</sub> carrier. Maintenance of viscosity is necessary to preserve shear stress on the vascular wall that prevents loss of the functional capillary density (123, 165). The viscosity and COP of PEG(HSA-FeP2) were modulated to some degree by changing the molecular weight of PEG [M<sub>w</sub>: 2 × 10<sup>3</sup> (PEG<sub>M2</sub>) and 5 × 10<sup>3</sup> (PEG<sub>M5</sub>)] (Figure 14b). In fact, PEG<sub>M2</sub>(HSA-FeP2) showed almost identical values of viscosity and COP to those of the nonmodified HSA-FeP2. In contrast, PEG<sub>M5</sub>(HSA-FeP2) showed a higher viscosity and more pronounced hyperoncotic property relative to those of HSA-FeP2. Nevertheless, PEG<sub>M5</sub> conjugate may be useful as an efficient plasma expander (118, 166).

Under physiological conditions, PEG<sub>Mn</sub>(HSA-FeP2) binds and releases O<sub>2</sub>. The P<sub>50</sub>(O<sub>2</sub>) values were almost identical to those of the original HSA-FeP2, indicating that the O<sub>2</sub> binding equilibrium was not influenced by the presence of the PEG chains (Figure 14b). Surface modification by PEG delays proton-driven oxidation of the O<sub>2</sub> adduct complex, giving HSA-FeP2 the τ<sub>1/2</sub>(O<sub>2</sub>) of 12 h, which is almost equal to that of a natural hemoprotein, Mb [τ<sub>1/2</sub>(O<sub>2</sub>), 12 h; pH 7, 35 °C] (167). The conjugated PEG might change the local proton concentration of the HSA interior compared to the outer aqueous solution.

The circulation persistence of FeP2 in the bloodstream was measured after administration of PEG<sub>Mn</sub>(HSA-FeP2) to anesthetized rats (164). The PEG<sub>Mn</sub>(HSA-FeP2) solution (20% volume of the circulatory blood) was injected intravenously into rats from the tail vein. The concentration decays of PEG<sub>Mn</sub>(HSA-FeP2) in the blood showed single exponentials with half-life [τ<sub>1/2</sub>(FeP2)] of 13–16 h (Figure 14c). These values are considerably longer than those of the corresponding nonmodified HSA-FeP1 (168). Surface modification of HSA-FeP2 by PEG prevented the rapid clearance of the incorporated FeP2. On the basis of these findings, we can conclude that surface modification of HSA-FeP2 by PEG comprehensively improved its O<sub>2</sub> transporting ability.

We then proceeded to evaluate physiological responses to an exchange transfusion with PEG<sub>M2</sub>(HSA-FeP2) in an acute anemia rat model (169) (Figure 15). The animals were first placed in a 65 vol % hemodilution with 5 g/dL HSA. They subsequently underwent a 30 vol % blood replacement with the PEG<sub>M2</sub>(HSA-FeP2) solution. As negative and positive control groups, a 5 g/dL HSA solution (HSA group) and washed RBC suspension (RBC group) were infused, respectively, to similarly operated rats in hemorrhage. The isovolemic 65% hemodilution with HSA reduced the Hb concentration, thereby decreasing the O<sub>2</sub> supply to the tissue. Consequently, the mean arterial pressure (MAP), renal cortical O<sub>2</sub> partial pressure [PtO<sub>2</sub>(R)], and O<sub>2</sub> partial pressure of muscle tissue [PtO<sub>2</sub>(M)] were decreased. During hemorrhagic shock by 30% bleeding, significant decreases in the MAP, venous O<sub>2</sub> pressure (PvO<sub>2</sub>), PtO<sub>2</sub>(R), and PtO<sub>2</sub>(M) were observed by the loss of the circulation blood volume. The heart rate (HR) and respiration rate were also decreased. In contrast, arterial O<sub>2</sub> pressure (PaO<sub>2</sub>) increased to about 160% of the basal value (b.v.). The arterial CO<sub>2</sub> pressure (PaCO<sub>2</sub>) decreased to about 62% of the b.v.; the pH increased to 7.55.

The injection of the sample solutions increased the blood volume and improved the circulatory flow. Lactate was washed out from the tissues and into the circulatory system, which decreased the pH to the initial level of 7.43 in all groups. The administration of HSA restored no parameters: death occurred within 41 min. In contrast, the infusion of PEG<sub>M2</sub>(HSA-FeP2) or RBC kept all the rats alive until the end of measurements. After injection of PEG<sub>M2</sub>(HSA-FeP2), the animals showed marked and rapid recovery in MAP, HR, PaO<sub>2</sub>, PvO<sub>2</sub>, PaCO<sub>2</sub>, and pH, resembling that shown in the RBC group. These results demonstrate the O<sub>2</sub> transporting capability of the PEG<sub>M2</sub>(HSA-FeP2) solution as a resuscitative fluid. We observed that albumin-based oxygen carrier does not induce hypertensive action, because of its low permeability through the vascular endothelium in comparison with that of Hb molecules. The heart rate responses after the injection were also negligibly small. Visualization of the intestinal microcirculatory changes clearly

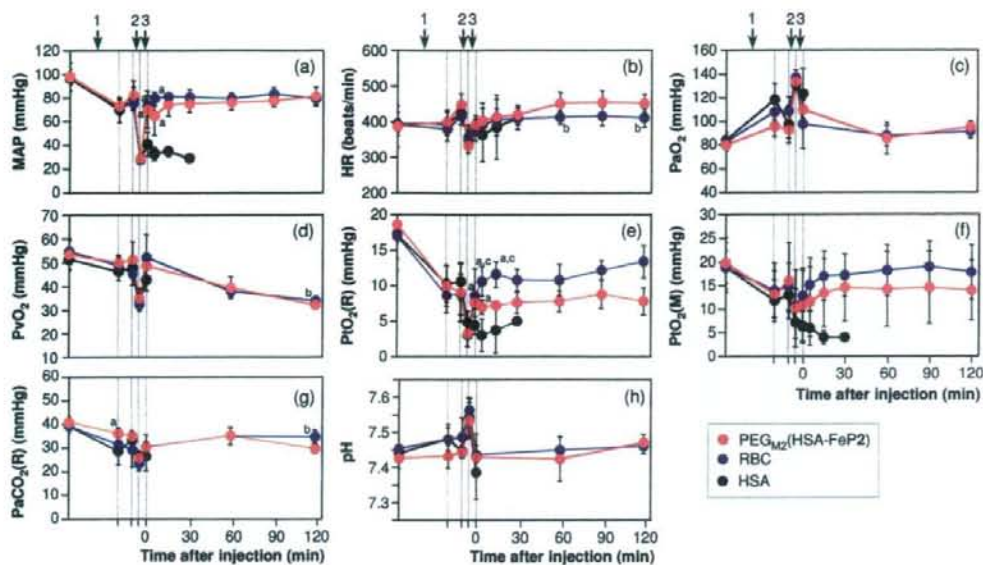


**Figure 15.** Effect of PEG<sub>M2</sub>(HSA-FeP2) solutions on (a) MAP, (b) HR, (c) PaO<sub>2</sub>, (d) PvO<sub>2</sub> (e) PtO<sub>2</sub>(R), (f) PtO<sub>2</sub>(M), (g) PaCO<sub>2</sub>, and (h) pH in anesthetized rats subjected to hemodilution and hemorrhage. Each value represents the mean  $\pm$  SD of five rats [red, PEG<sub>M2</sub>(HSA-FeP2) group; blue, washed RBC group; and black, HSA group]. Arrows (1), (2), and (3), respectively, indicate the periods of 65% hemodilution, 30% bleeding, and sample infusion. <sup>a</sup>*p* < 0.05 versus HSA group (Tukey-Kramer test), <sup>b</sup>*p* < 0.05 versus PEG<sub>M2</sub>(HSA-FeP2) group (unpaired *t*-test), and <sup>c</sup>*p* < 0.05 versus PEG<sub>M2</sub>(HSA-FeP2) group (Tukey-Kramer test).

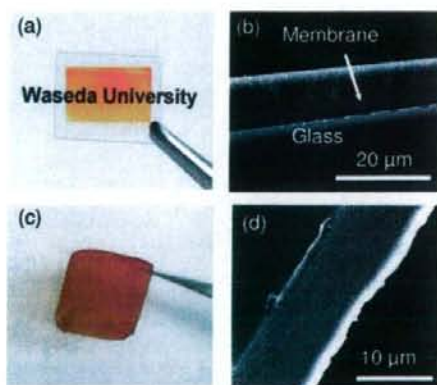


**Figure 16.** The solid membrane of PEG<sub>M2</sub>(HSA-FeP). (a) Photograph of the membrane on the glass, (b) SEM of the membrane section, (c) photograph of the flexible film peeled from the poly(styrene) dish, and (d) SEM of the isolated film.

revealed the widths of the venule and arteriole to be fairly constant (170).

Reversible oxygenation of PEG<sub>M2</sub>(HSA-FeP2) was observed even in the solid state (171). The aqueous solution of PEG<sub>M2</sub>(HSA-FeP2(CO)) complex was spread on the glass plate and dried overnight at room temperature, producing a red transparent solid membrane (Figure 16a). In contrast, HSA-FeP2 without PEG decoliation yielded a brittle membrane with many cracks. Scanning electron microscopy (SEM) observations of the PEG<sub>M2</sub>(HSA-FeP2) membrane showed a uniform thickness of 15  $\mu$ m and a smooth surface (Figure 16b). The  $\tau_{1/2}(O_2)$  was 40 h, which is three times longer than the value in water. The O<sub>2</sub> binding affinity was about a half that of the monomeric PEG<sub>M2</sub>(HSA-FeP2).

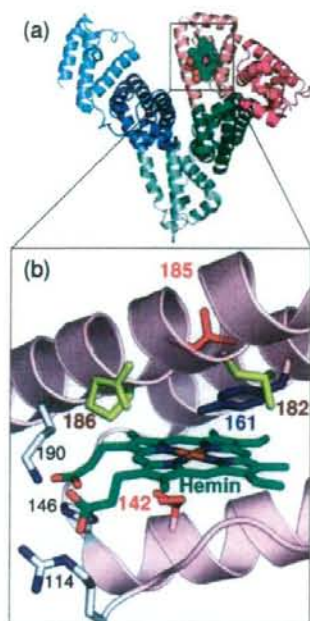
We subsequently added hyaluronic acid (HA) as a supporting polymer to the protein solution and prepared the solid membrane

on a poly(styrene) dish. Actually, HA is known as a glycosaminoglycan component of connective tissues, hyaline bodies, and extracellular matrix (172). Water evaporation of the PEG<sub>M2</sub>(HSA-FeP2)/HA mixture ([HSA]: 2.5 wt % and [HA]: 0.2 wt %) produced a uniform red solid membrane that was easily peeled from the dish, yielding a free-standing homogeneous thin film of the PEG(HSA-FeP2)/HA hybrid (Figure 16c,d).

The PEG<sub>M2</sub>(HSA-FeP2) solution is useful as a valuable O<sub>2</sub>-carrying plasma. Membranes of PEG<sub>M2</sub>(HSA-FeP2) with micrometer thickness can serve as a RBC substitute that can be preserved anywhere and reproduced as a saline solution at any time.

**3.3. Recombinant HSA-Heme (rHSA-Heme) Prepared Using Site-Directed Mutagenesis.** Hemin [Fe<sup>3+</sup> protoporphyrin IX] released from metHb during enucleation of RBC or through hemolysis is captured by HSA with a high binding constant ( $K \approx 10^8 \text{ M}^{-1}$ ) (173). Crystallographic studies have revealed that heme is bound within a narrow D-shaped hydrophobic cavity in subdomain IB with axial coordination of Tyr-161 to the central ferric ion and electrostatic interactions between the porphyrin propionates and a triad of basic amino acid residues (Arg-114, His-146, and Lys-190) (Figure 17) (174, 175). In terms of the general hydrophobicity of this  $\alpha$ -helical heme pocket, the subdomain IB of HSA potentially has similar features to the heme binding site of Hb or Mb. However, when one reduces HSA-hemin to obtain the ferrous complex, it is autoxidized rapidly by O<sub>2</sub>, even at low temperature ( $\sim 0^\circ \text{C}$ ), because HSA lacks the proximal His, which, in Hb and Mb, enables the prosthetic heme group to bind O<sub>2</sub>. Knowledge of the detailed architecture of the heme binding site in HSA enables us to design mutagenesis experiments to construct a tailor-made heme pocket for stable O<sub>2</sub> binding. Therefore, we used site-directed mutagenesis to introduce an His into the heme binding site that was expected to provide axial coordination to the central Fe<sup>2+</sup> atom of the heme and thereby promote O<sub>2</sub> binding.

Results of our modeling experiments suggested that a favorable position for the axial imidazole insertion would be Ile-142 (Figure 17). The N <sub>$\epsilon$</sub> (His)-Fe distances were estimated



rHSA-heme	Position				
	142	161	182	185	186
Wild type	Ile	Tyr	Leu	Leu	Arg
I142H	<b>His</b>	Tyr	Leu	Leu	Arg
I142H/Y161L (HL)	<b>His</b>	<b>Leu</b>	Leu	Leu	Arg
I142H/Y161F (HF)	<b>His</b>	<b>Phe</b>	Leu	Leu	Arg
HL/L185N	<b>His</b>	<b>Leu</b>	Leu	<b>Asn</b>	Arg
HF/L185N	<b>His</b>	<b>Phe</b>	Leu	<b>Asn</b>	Arg
HL/L185Q	<b>His</b>	<b>Leu</b>	Leu	<b>Gln</b>	Arg
HF/L185Q	<b>His</b>	<b>Phe</b>	Leu	<b>Gln</b>	Arg
HF/L185H	<b>His</b>	<b>Phe</b>	Leu	<b>His</b>	Arg
HL/R186L	<b>His</b>	<b>Leu</b>	Leu	Leu	<b>Leu</b>
HL/R186F	<b>His</b>	<b>Leu</b>	Leu	Leu	<b>Phe</b>

**Figure 17.** (a) Crystal structure of HSA-hemin complex (1O9X) from ref 174. Hemin is shown in a space-filling representation. (b) Heme pocket structure in subdomain IB and positions of amino acids where site-specific mutations were introduced. Abbreviations of rHSA(mutant)s are shown in the table.

as 2.31 Å for H142 (compared to 2.18 Å for Mb). We therefore designed and produced two single mutants I142H and a double mutant I142H/Y161L (HL) (176).

In the UV-vis absorption spectrum of rHSA(HL)-hemin, the ligand-to-metal charge transfer band at 625 nm was weakened because of the Y161L mutation. The MCD spectrum of rHSA(HL)-hemin showed a similar S-shaped pattern in the Soret band region resembling that of ferric Mb (177, 178). These results suggest that rHSA(HL)-hemin is in a predominantly ferric high-spin complex having a water molecule as the sixth ligand. The rHSA-hemin was easily reduced to the ferrous complex by adding a small molar excess of aqueous sodium dithionite under an Ar atmosphere (Figure 18). A single broad absorption band ( $\lambda_{\text{max}}$ : 559 nm) in the visible absorption spectrum and the MCD spectrum of rHSA(HL)-heme indicated the formation of a five-N-coordinate high-spin complex (176, 177, 179). The heme therefore appears to be accommodated in the mutated heme pocket with an axial coordination involving His-142. Upon exposure of rHSA(HL)-heme solution to O<sub>2</sub>, the UV-vis absorption changed immediately to that of the O<sub>2</sub> adduct complex (Figure 18). It formed a carbonyl complex under a CO atmosphere. The single mutant rHSA(I142H)-heme, which retains Y161, was unable to bind O<sub>2</sub>. The polar phenolate residue at the top of the porphyrin plane is likely to accelerate the proton-driven oxidation of the Fe<sup>2+</sup> center. The replacement of Tyr-161 in rHSA(I142H)-heme by Leu enhanced stabilization of the O<sub>2</sub> adduct complex.

To evaluate the kinetics of O<sub>2</sub> and CO bindings to rHSA-hemes, laser flash photolysis experiments were carried out (Tables 7 and 8). It is noteworthy that the absorbance decay accompanying the CO recombination to rHSA(HL)-heme was composed of double-exponential profiles, which is normally not observed in Mb (the faster phase is defined as species I; the slower phase is defined as species II). The ratio of the amplitude of the species I and the species II was approximately 3:2. On the other hand, the rebinding of O<sub>2</sub> to rHSA(HL)-heme followed a simple monophasic decay. Numerous investigations of syn-

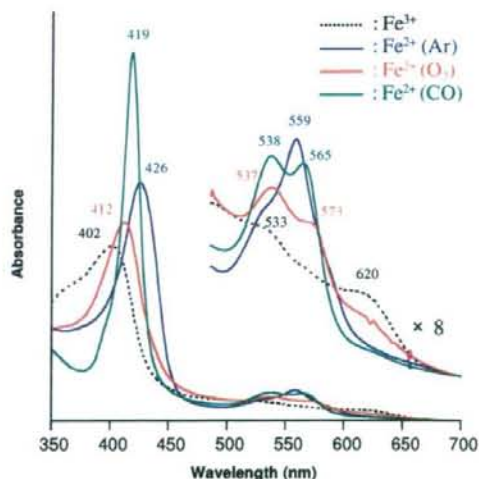


**Figure 18.** UV-vis absorption spectral changes of rHSA(HL)-heme in potassium phosphate buffered solution (pH 7.0).

thetic model hemes have helped to reveal the relation between the structure around the hemes and their O<sub>2</sub> and CO binding abilities (4, 147, 148). A bending strain in the proximal base coordination to the central Fe<sup>2+</sup> atom, the “proximal-side steric (proximal pull) effect”, is known to be capable of both increasing the dissociation rate for CO and decreasing the association rate. Simultaneously, it increases the O<sub>2</sub> dissociation rate without greatly altering the O<sub>2</sub> association kinetics. Consequently, one possible explanation for the existence of the two phases is that two different geometries of the axial His (His-142) coordination to the central ferrous ion of the heme might exist, each one accounting for a component of the biphasic kinetics of CO rebinding.

**Table 7. O<sub>2</sub> Binding Parameters of rHSA(Mutant)-Heme Complexes in Phosphate Buffered Solution (pH 7.0) at 22 °C**

hemoproteins	$k_{on}(O_2)$ ( $\mu M^{-1} s^{-1}$ )	$k_{off}(O_2)$ (m s <sup>-1</sup> )		$P_{50}(O_2)$ (Torr)	
		I	II	I	II
rHSA(HL)-heme	7.5	0.22	1.70	18	134
rHSA(HF)-heme	20	0.10	0.99	3	31
rHSA(HL/L185N)-heme	14	0.02	0.29	1	14
rHSA(HF/L185N)-heme	26	0.10	1.03	2	24
rHSA(HL/R186L)-heme	25	0.41	8.59	10	209
rHSA(HL/R186F)-heme	21	0.29	7.01	9	203
Mb <sup>a</sup>	14	0.012		0.51	
RBC <sup>b</sup>				8	

<sup>a</sup> Sperm whale myoglobin in 0.1 M potassium phosphate buffer (pH 7.0, 20 °C); ref 180. <sup>b</sup> Human red cell suspension in isotonic buffer (pH 7.4, 20 °C); ref 181.

**Table 8. CO Binding Parameters of rHSA(Mutant)-Heme Complexes in Phosphate Buffered Solution (pH 7.0) at 22 °C**

hemoproteins	$k_{on}(CO)$ ( $\mu M^{-1} s^{-1}$ )		$k_{off}(CO)$ (s <sup>-1</sup> )		$P_{50}(CO)$ (Torr)	
	I	II	I	II	I	II
rHSA(HL)-heme	2.0	0.27	0.013	0.079	0.0053	0.240
rHSA(HF)-heme	6.8	0.72	0.009	0.061	0.0011	0.068
rHSA(HL/L185N)-heme	6.8	1.60	0.008	0.039	0.0010	0.020
rHSA(HF/L185N)-heme	7.7	1.09	0.008	0.043	0.0008	0.032
rHSA(HL/R186L)-heme	5.0	0.57	0.011	0.165	0.0018	0.234
rHSA(HL/R186F)-heme	7.9	1.12	0.010	0.148	0.0010	0.107
Mb <sup>a</sup>	0.51		0.019		0.03	

<sup>a</sup> Sperm whale myoglobin in 0.1 M potassium phosphate buffer (pH 7.0, 20 °C); ref 180.

**3.4. Modulation of O<sub>2</sub> Binding Property of rHSA(mutant)-Heme.** To control the O<sub>2</sub> binding affinity of rHSA-heme, we designed and produced diverse rHSA(mutant)-hemes in which bulky hydrophobic or hydrophilic amino acids were introduced around the O<sub>2</sub> binding site (Tyr-161, Leu-182, Leu-185, and Arg-186) (Figure 17). More recently, the beneficial effect of low-dose CO on the microcirculation by a hemoglobin-based artificial oxygen carrier has been discussed (132, 182). Control of the CO binding affinity of rHSA-heme is also tempting.

**A. Substitution of Tyr-161 with Leu or Phe.** The first, Tyr-161, was substituted to noncoordinating and hydrophobic amino acids (Leu or Phe). The O<sub>2</sub> and CO binding properties of rHSA(HL)-heme and rHSA(I142H/Y161F)-heme [rHSA(HF)-heme] showed that the presence of a Phe rather than a Leu at position 161 results in 6-fold and 4-fold increases in the O<sub>2</sub> binding affinity for species I and II, respectively (Table 7). This enhancement is mainly attributable to an increase in the O<sub>2</sub> association rate constant. The same trend was observed for CO binding [3-fold increase in  $k_{on}(CO)$ ] (Table 8). The substitution of Leu-161 (102 Å<sup>3</sup>) by Phe-161 (137 Å<sup>3</sup>) (183) replaces an isopropyl group with a rigid benzyl group within the heme pocket. In rHSA(HL), the small side chain of Leu-161 might enable free rotation of the side chain of neighboring Leu-185, thereby reducing the volume on the distal side of the porphyrin plane (Figure 19a,b). On the other hand, the bulkier aromatic side chain of Phe-161 might prevent rotation of the isopropyl group of Leu-185 and thereby provide greater room of the distal pocket; this effect might provide easier access to the heme Fe<sup>2+</sup> atom and account for the increased association rates for O<sub>2</sub> and CO.

**B. Substitution of Leu-185 with Polar Amino Acid.** Leu-185 was substituted with a more hydrophilic amino acid (Asn, Gln, or His), which was expected to interact with the coordinated O<sub>2</sub> by hydrogen bond and to stabilize the O<sub>2</sub> adduct complex similarly to Hb and Mb. In rHSA(mutant)-hemes in which Gln

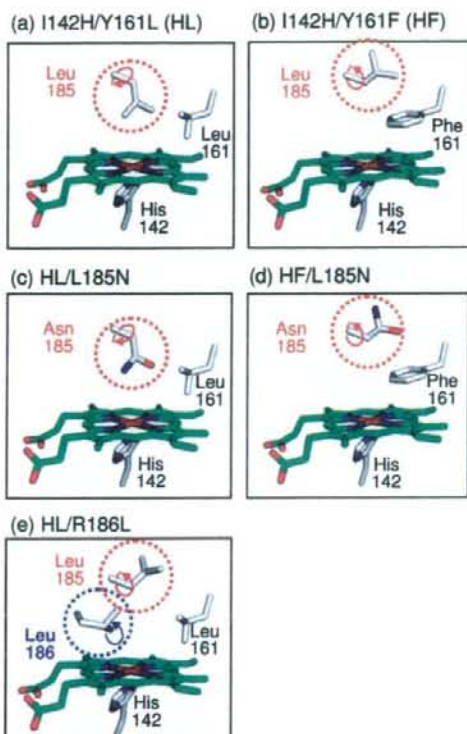


**Figure 19.** The proposed configuration of Leu-185 in (a) rHSA(HL)-heme and (b) rHSA(HF)-heme, Asn-185 in (c) rHSA(HL/L185N)-heme and (d) rHSA(HF/L185N)-heme, and Leu-186 in (e) rHSA(HL/R186L)-heme.

or His was introduced into Leu-185, they formed ferrous six-coordinated low-spin complexes under an Ar atmosphere. That result suggests that the introduced amino acid coordinates to the heme iron as a sixth ligand under an Ar atmosphere. Upon exposure of the solutions to O<sub>2</sub>, they were oxidized. Bis-histidyl hemochromes are known to be oxidized by O<sub>2</sub> rapidly via an outer sphere mechanism (184–186). On the other hand, rHSA(HL/L185N)-heme and rHSA(HF/L185N)-heme in which Asn was introduced at Leu-185 formed ferrous five-coordinated high-spin complexes under an Ar atmosphere. They formed O<sub>2</sub> adduct complexes under O<sub>2</sub> atmosphere. The introduced Asn is estimated to be too far to coordinate to the heme.

Marked differences were apparent in a comparison of the O<sub>2</sub> and CO binding parameters for rHSA(HL)-heme and rHSA(HL/L185N)-heme. First, the presence of Asn rather than Leu at position 185 caused 2-fold and 3–6-fold increases, respectively, in the  $k_{on}(O_2)$  and  $k_{on}(CO)$  values. The Asn might partly rotate upward, which provides somewhat greater space of the distal pocket. Second, Asn-185 induced 18-fold and 10-fold increases in the O<sub>2</sub> binding affinity for species I and II, because the  $k_{off}(O_2)$  values were 1/6–1/11 of their former values. This corresponds to a free energy difference of  $-1.8$  kcal mol<sup>-1</sup> at 22 °C. The magnitude of the effect seems to be reasonable considering that, in HbO<sub>2</sub> and MbO<sub>2</sub>, the distal His-64 stabilizes the coordinated O<sub>2</sub> by  $-0.6$  to  $-1.4$  kcal mol<sup>-1</sup> because of the hydrogen bond (187). In contrast, the O<sub>2</sub> and CO binding parameters for rHSA(HF)-heme and rHSA(HF/L185N)-heme showed no significant differences. The bulky benzyl side chain of Phe-161 can prevent rotation of the polar amide group of Asn-185 and thereby decrease the effect of polarity and size on O<sub>2</sub> and CO binding parameters (Figure 19c,d) (188).